

Topological Weyl Semimetal and Unconventional Superconductivity in Doped Topological Insulators

万贤纲 (Xiangang Wan)

南京大学物理系

2013年11月13日

清华高研院

内 容

□Weyl半金属

□BiS₂超导体

□掺杂拓扑绝缘体

合作者

Sergej Savrasov, UC Davis



Ari Turner & Ashvin Vishvanath
UC Berkeley



段纯刚

华东师大

曹刚

肯塔基大学

Qiang Wang, Daniel S Dessa

科罗拉多大学/橡树岭

动机(5d元素)

PERIODIC TABLE OF THE ELEMENTS

<http://www.ktf-split.hr/periodni/en/>

PERIODIC TABLE OF THE ELEMENTS

<http://www.ktf-split.hr/periodni/en/>

Legend:

- Metal
- Semimetal
- Nonmetal
- Alkali metal
- Alkaline earth metal
- Transition metals
- Chalcogens element
- Halogens element
- Noble gas
- Lanthanide
- Actinide

STANDARD STATE (25 °C; 101 kPa)

- Ne - gas
- Fe - solid
- Ga - liquid
- Tc - synthetic

GROUP	1 IA	2 IIA	3 IIA	4 IVA	5 VA	6 VIA	7 VIIA	8 VIIIA										
PERIOD 1	1 1.0079 H HYDROGEN	2 9.0122 Be BERYLLIUM	13 10.811 B BORON	14 12.011 C CARBON	15 14.007 N NITROGEN	16 15.999 O OXYGEN	17 18.998 F FLUORINE	18 4.0026 He HELIUM										
PERIOD 2	3 6.941 Li LITHIUM	4 9.0122 Be BERYLLIUM	5 10.811 B BORON	6 12.011 C CARBON	7 14.007 N NITROGEN	8 15.999 O OXYGEN	9 18.998 F FLUORINE	10 20.180 Ne NEON										
PERIOD 3	11 22.990 Na SODIUM	12 24.305 Mg MAGNESIUM	13 10.811 B BORON	14 12.011 C CARBON	15 13.998 P PHOSPHORUS	16 32.065 S SULPHUR	17 35.453 Cl CHLORINE	18 39.948 Ar ARGON										
PERIOD 4	19 39.098 K POTASSIUM	20 40.078 Ca CALCIUM	21 44.956 Sc SCANDIUM	22 47.867 Ti TITANIUM	23 50.942 V VANADIUM	24 51.996 Cr CHROMIUM	25 54.938 Mn MANGANESE	26 55.845 Fe IRON	27 58.933 Co COBALT	28 58.693 Ni NICKEL	29 63.546 Cu COPPER	30 65.39 Zn ZINC	31 69.723 Ga GALLIUM	32 72.64 Ge GERMANIUM	33 74.922 As ARSENIC	34 78.96 Se SELENIUM	35 79.904 Br BROMINE	36 83.80 Kr KRYPTON
PERIOD 5	37 85.468 Rb RUBIDIUM	38 87.62 Sr STRONTIUM	39 88.906 Y YTTRIUM	40 91.224 Zr ZIRCONIUM	41 92.906 Nb NIOBIUM	42 95.94 Mo MOLYBDENUM	43 (98) Tc TECHNETIUM	44 101.07 Ru RUTHENIUM	45 102.91 Rh RHODIUM	46 106.42 Pd PALLADIUM	47 107.87 Ag SILVER	48 112.41 Cd CADMIUM	49 114.82 In INDIUM	50 118.71 Sn TIN	51 121.76 Sb ANTIMONY	52 127.60 Te TELLURIUM	53 126.90 I IODINE	54 131.29 Xe XENON
PERIOD 6	55 132.91 Cs CAESIUM	56 137.33 Ba BARIUM	57-71 La-Lu Lanthanide	72 178.49 Hf HAFNIUM	3 180.95 Ta	74 183.84 W	75 186.21 Re	76 190.23 Os	77 192.22 Ir	78 195.0 Pt	79 196.97 Au GOLD	80 200.59 Hg MERCURY	81 204.38 Tl THALLIUM	82 207.2 Pb LEAD	83 208.98 Bi BISMUTH	84 (209) Po POLONIUM	85 (210) At ASTATINE	86 (222) Rn RADON
PERIOD 7	87 (223) Fr FRANCIUM	88 (226) Ra RADIUM	89-103 Ac-Lr Actinide	104 (261) Rf RUTHERFORDIUM	105 (262) Db DUBNIUM	106 (266) Sg SEABORGIUM	107 (264) Bh BOHRIUM	108 (277) Hs HASSIUM	109 (268) Mt MEITNERIUM	110 (281) Uum UNUNNILIUM	111 (272) Uuu UNUNUNIUM	112 (285) Uub UNUNBIIUM	114 (289) Uuq UNUNQUADMIUM					

LANTHANIDE

57 138.91 La LANTHANUM	58 140.12 Ce CERIUM	59 140.91 Pr PRASEODYMIUM	60 144.24 Nd NEODYMIUM	61 (145) Pm PROMETHIUM	62 150.36 Sm SAMARIUM	63 151.96 Eu EUROPIUM	64 157.25 Gd GADOLINIUM	65 158.93 Tb TERBIUM	66 162.50 Dy DYSPROSIUM	67 164.93 Ho HOLMIUM	68 167.26 Er ERBIUM	69 168.93 Tm THULIUM	70 173.04 Yb YTTERBIUM	71 174.97 Lu LUTETIUM
-------------------------------------	----------------------------------	--	-------------------------------------	-------------------------------------	------------------------------------	------------------------------------	--------------------------------------	-----------------------------------	--------------------------------------	-----------------------------------	----------------------------------	-----------------------------------	-------------------------------------	------------------------------------

ACTINIDE

89 (227) Ac ACTINIUM	90 232.04 Th THORIUM	91 231.04 Pa PROTACTINIUM	92 238.03 U URANIUM	93 (237) Np NEPTUNIUM	94 (244) Pu PLUTONIUM	95 (243) Am AMERICIUM	96 (247) Cm CURIUM	97 (247) Bk BERKELIUM	98 (251) Cf CALIFORNIUM	99 (252) Es EINSTEINIUM	100 (257) Fm FERMIUM	101 (258) Md MENDELEVIUM	102 (259) No NOBELIUM	103 (262) Lr LAWRENCIUM
-----------------------------------	-----------------------------------	--	----------------------------------	------------------------------------	------------------------------------	------------------------------------	---------------------------------	------------------------------------	--------------------------------------	--------------------------------------	-----------------------------------	---------------------------------------	------------------------------------	--------------------------------------

(1) Pure Appl. Chem., 73, No. 4, 667-683 (2001)
Relative atomic mass is shown with five significant figures. For elements have no stable nuclides, the value enclosed in brackets indicates the mass number of the longest-lived isotope of the element.
However three such elements (Th, Pa, and U) do have a characteristic terrestrial isotopic composition, and for these an atomic weight is tabulated.

Copyright © 1998-2003 EniG. (eni@ktf-split.hr)

内容

5d过渡金属氧化物

- 烧绿石结构铱化合物
磁基态构型, Weyl半金属, Fermi Arc
- 设计Axion绝缘体
- Slater insulator
- BiS₂超导体
- 电声子耦合→非常规超导体
- 总结

5d过渡元素氧化物的特点 自旋轨道耦合和电子关联



www.sciencemag.org SCIENCE VOL 323 6 MARCH 2009

PRL 101, 076402 (2008)

PHYSICAL REVIEW LETTERS

Phase-Sensitive Observation of a Spin-Orbital Mott State in Sr_2IrO_4

B. J. Kim,^{1,2*} H. Ohsumi,³ T. Komesu,³ S. Sakai,^{3,4} T. Morita,^{3,5} H. Takagi,^{1,2*} T. Arima^{3,6}

Measurement of the quantum-mechanical phase in quantum matter provides the most direct manifestation of the underlying abstract physics. We used resonant x-ray scattering to probe the relative phases of constituent atomic orbitals in an electronic wave function, which uncovers the unconventional Mott insulating state induced by relativistic spin-orbit coupling in the layered 5d transition metal oxide Sr_2IrO_4 . A selection rule based on intra-atomic interference effects establishes a complex spin-orbital state represented by an effective total angular momentum = 1/2 quantum number, the phase of which can lead to a quantum topological state of matter.

Novel $J_{\text{eff}} = 1/2$ Mott State Induced by Relativistic Spin-Orbit Coupling

•尽管5d的实空间轨道半径很大，但是由于强的自旋轨道耦合，仍然有不可忽略的电子关联效应。

由于自旋轨道耦合和电子关联的联合效应导致了 Sr_2IrO_4 等5d⁵电子体系是绝缘体

5d⁵

强自旋轨道耦合下的T_{2g}轨道

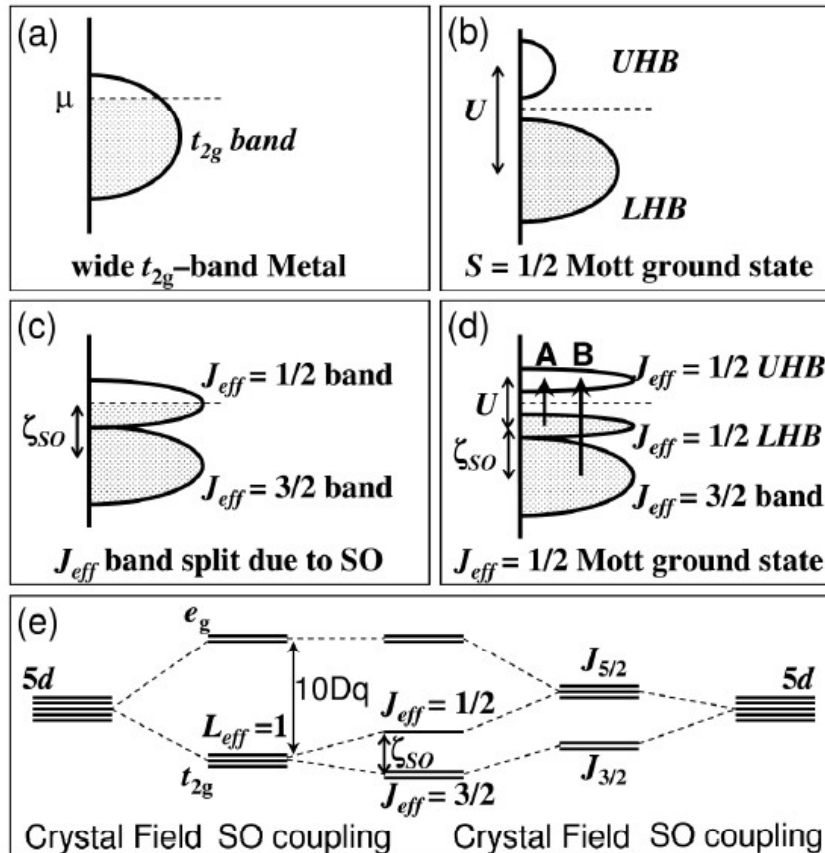
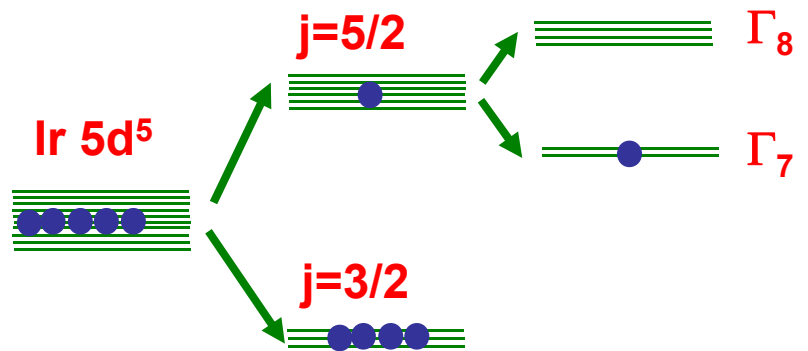


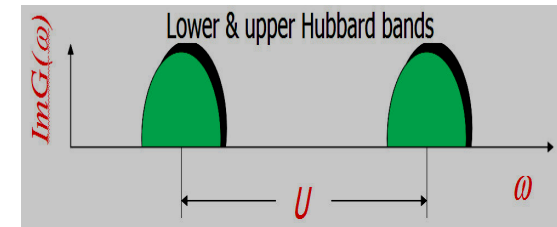
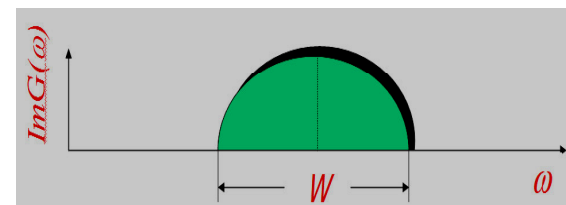
FIG. 1. Schematic energy diagrams for the 5d⁵ (t_{2g}^5) configuration (a) without SO and U, (b) with an unrealistically large U but no SO, (c) with SO but no U, and (d) with SO and U. Possible optical transitions A and B are indicated by arrows. (e) 5d level splittings by the crystal field and SO coupling.

(after Kim et.al, PRL 2009)

强晶体场下的相对论5d电子



A small Hubbard U produces Mott insulating behavior for Γ_7 band at half filling



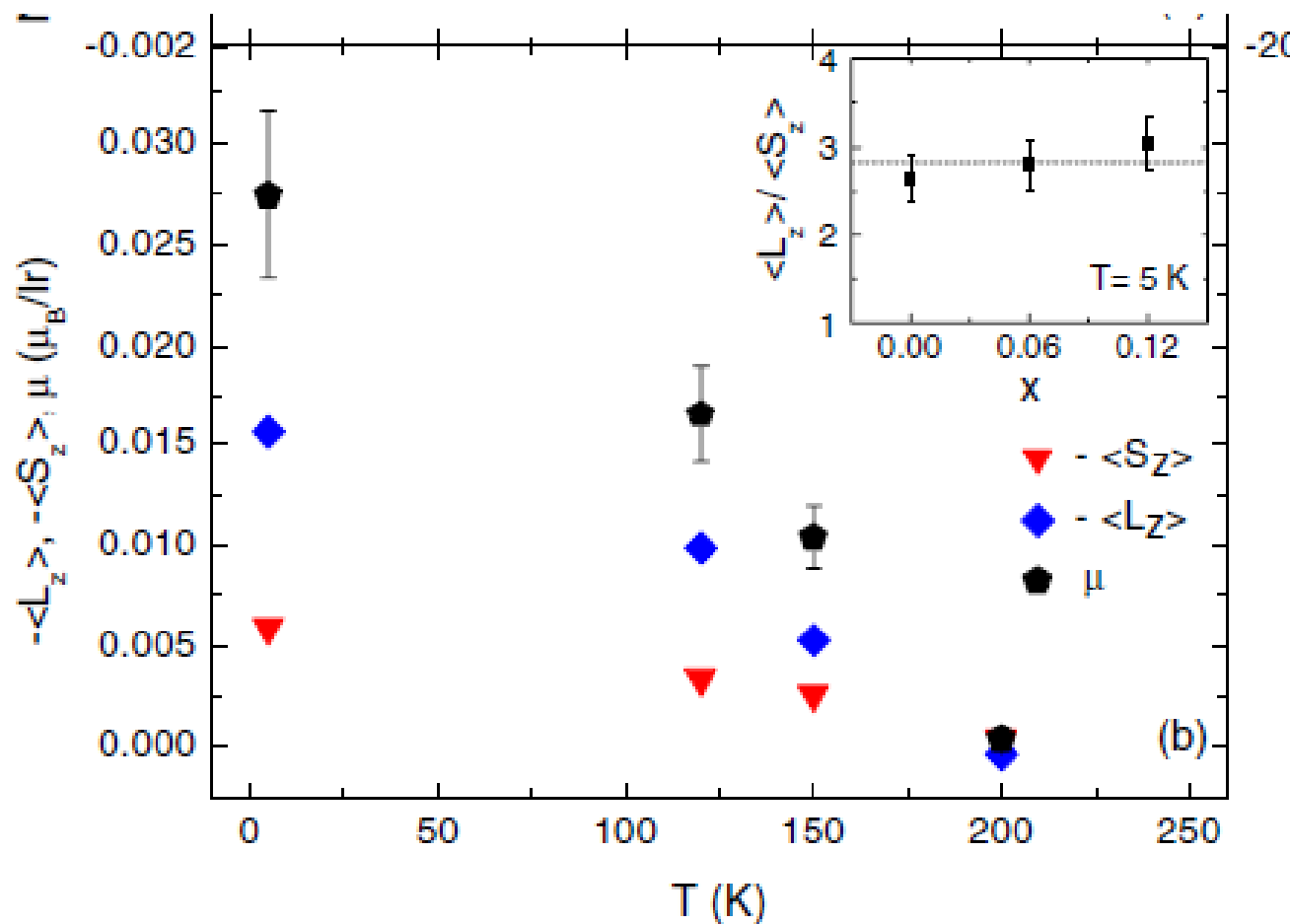
5d过渡元素氧化物的特点 强自旋轨道耦合

PRL 105, 216407 (2010)

PHYSICAL REVIEW LETTERS

week ending
19 NOVEMBER 2010

Orbital Magnetism and Spin-Orbit Effects in the Electronic Structure of BaIrO₃



5d过渡元素氧化物的特点

PRL 99, 137207 (2007)

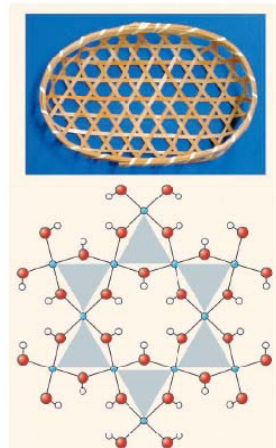
PHYSICAL REVIEW LETTERS

week e
28 SEPTEM

Spin-Liquid State in the $S = 1/2$ Hyperkagome Antiferromagnet $\text{Na}_4\text{Ir}_3\text{O}_8$

- 1) 有着**hyperkagome** 结构
- 2) Curie-Weiss 温度(大约为650K)
- 3) effective moment 也较大 ($1.96\mu_B$) ??
- 4) 在极低的温度下它都不表现任何磁有序。

三维的量子自旋液体?



An End to the Drought of Quantum Spin Liquids

After decades of searching, several promising examples of a new quantum state of matter have now emerged.

Patrick A. Lee

PRL 101, 197202 (2008)

PHYSICAL REVIEW LETTERS

week ending
7 NOVEMBER 2008

Gapless Spin Liquids on the Three-Dimensional Hyperkagome Lattice of $\text{Na}_4\text{Ir}_3\text{O}_8$

Michael J. Lawler,¹ Arun Paramekanti,¹ Yong Baek Kim,¹ and Leon Balents²

PRL 99, 037201 (2007)

PHYSICAL REVIEW LETTERS

week ending
20 JULY 2007

Classical Antiferromagnet on a Hyperkagome Lattice

John M. Hopkinson,¹ Sergei V. Isakov,¹ Hae-Young Kee,¹ and Yong Baek Kim^{1,2}

PRL 101, 197201 (2008)

PHYSICAL REVIEW LETTERS

week ending
7 NOVEMBER 2008

$\text{Na}_4\text{Ir}_3\text{O}_8$ as a 3D Spin Liquid with Fermionic Spinons

Yi Zhou,^{1,2} Patrick A. Lee,³ Tai-Kai Ng,⁴ and Fu-Chun Zhang¹

5d过渡元素氧化物的特点

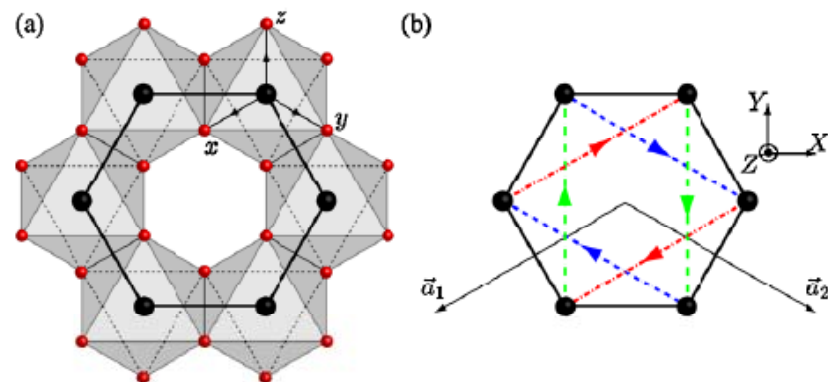
PRL 102, 256403 (2009)

PHYSICAL REVIEW LETTERS

week en
26 JUNE

Quantum Spin Hall Effect in a Transition Metal Oxide Na_2IrO_3

Atsuo Shitade,^{1,*} Hosho Katsura,² Jan Kuneš,^{3,4} Xiao-Liang Qi,⁵ Shou-Cheng Zhang,⁵ and Naoto Nagaosa^{1,2}



Mott Insulators in the Strong Spin-Orbit Coupling Limit: From Heisenberg to a Quantum Compass and Kitaev Models

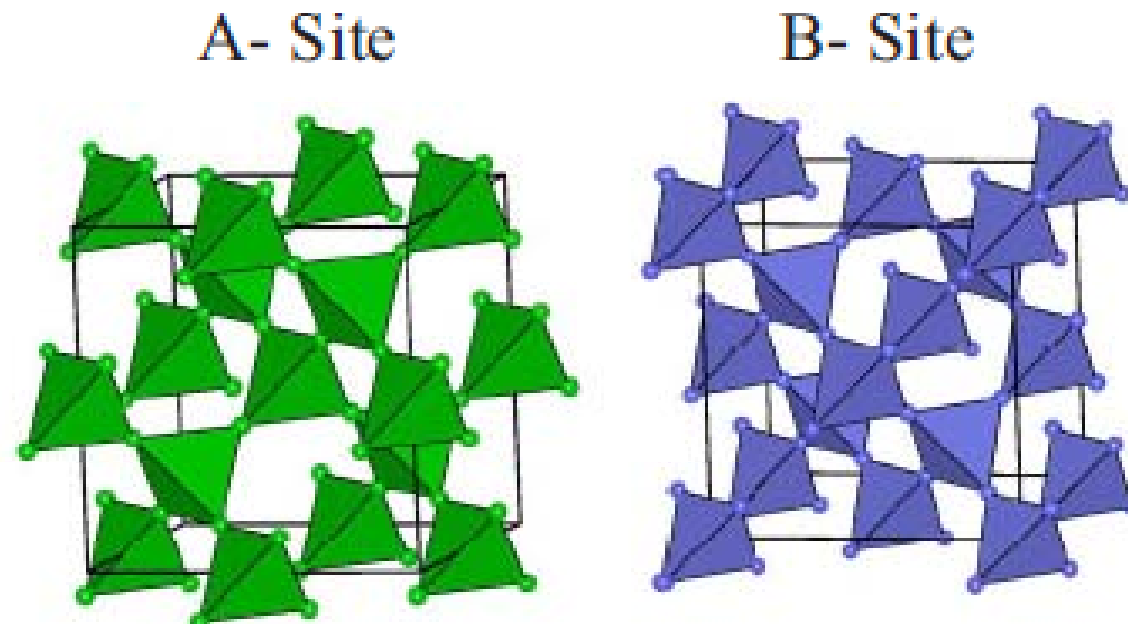
G. Jackeli^{1,*} and G. Khaliullin¹

PRL 102, 017205 (2009)

实验证实它有长程磁序 (Singh and Gegenwart 2010)

烧绿石结构 磁阻错现象

烧绿石结构 $\mathbf{A_2B_2O_7}$; 尖晶石结构 $\mathbf{AB_2O_4}$

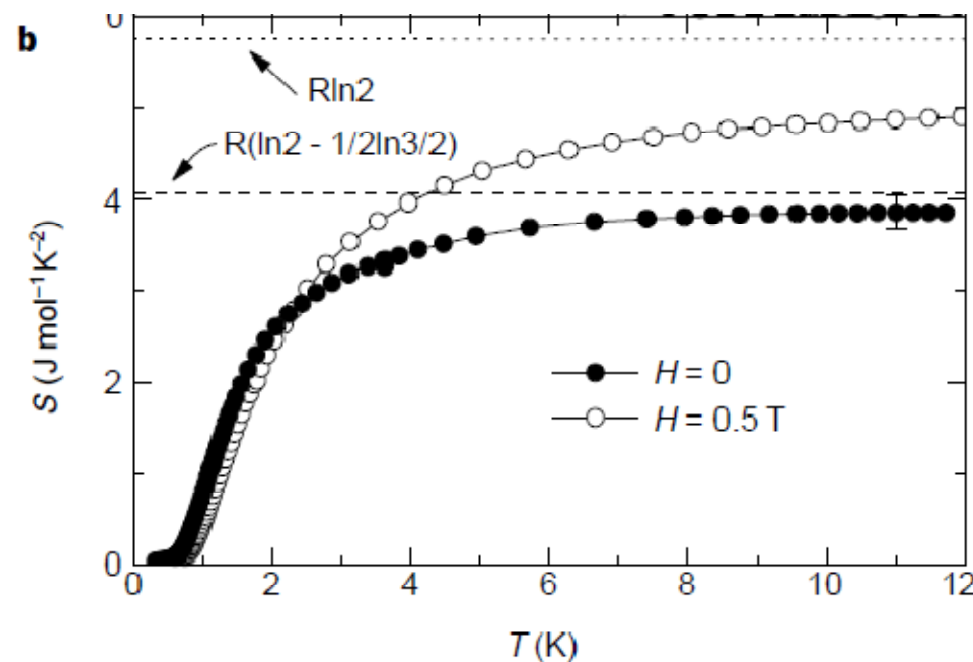


Spin ice

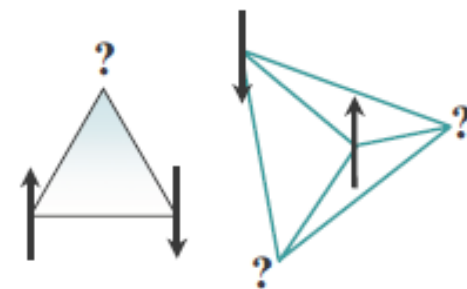
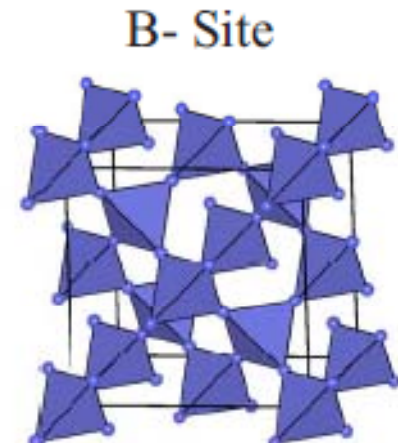
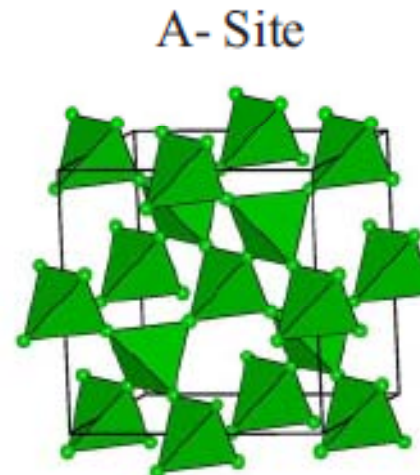
$A_2B_2O_7$,部分4f元素占据A位时表现出Ising-type的各向异性。

当铁磁的exchange interaction和Ising-type的各向异性结合可以导致出巨大的Geometrical frustration

NATURE | VOL 399 | 27 MAY 1999 | www.nature.com



$Ho_2Ti_2O_7$

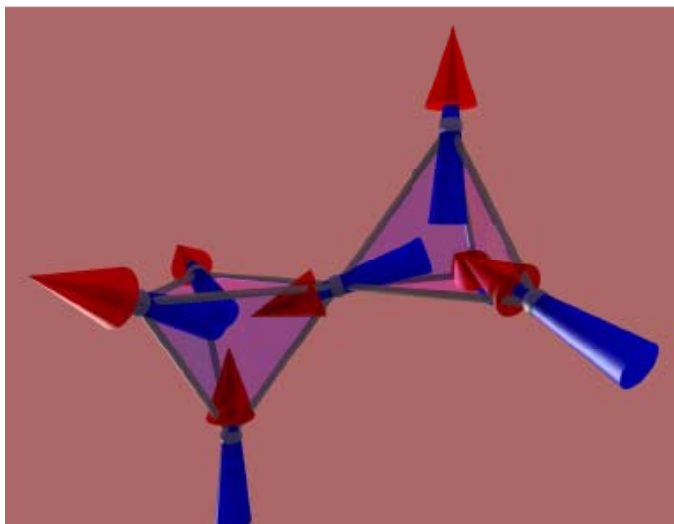


Magnetic Monopoles in Spin Ice

$$H = \frac{J}{3} \sum_{\langle ij \rangle} S_i S_j + D a^3 \sum_{(ij)} \left[\frac{\hat{e}_i \cdot \hat{e}_j}{|\mathbf{r}_{ij}|^3} - \frac{3(\hat{e}_i \cdot \mathbf{r}_{ij})(\hat{e}_j \cdot \mathbf{r}_{ij})}{|\mathbf{r}_{ij}|^5} \right] S_i S_j$$



$$\mathcal{V}(r_{ij}) = \begin{cases} \frac{\mu_0}{4\pi} \frac{q_i q_j}{r_{ij}} & r_{ij} \neq 0 \\ v_0 q_i q_j & r_{ij} = 0, \end{cases}$$

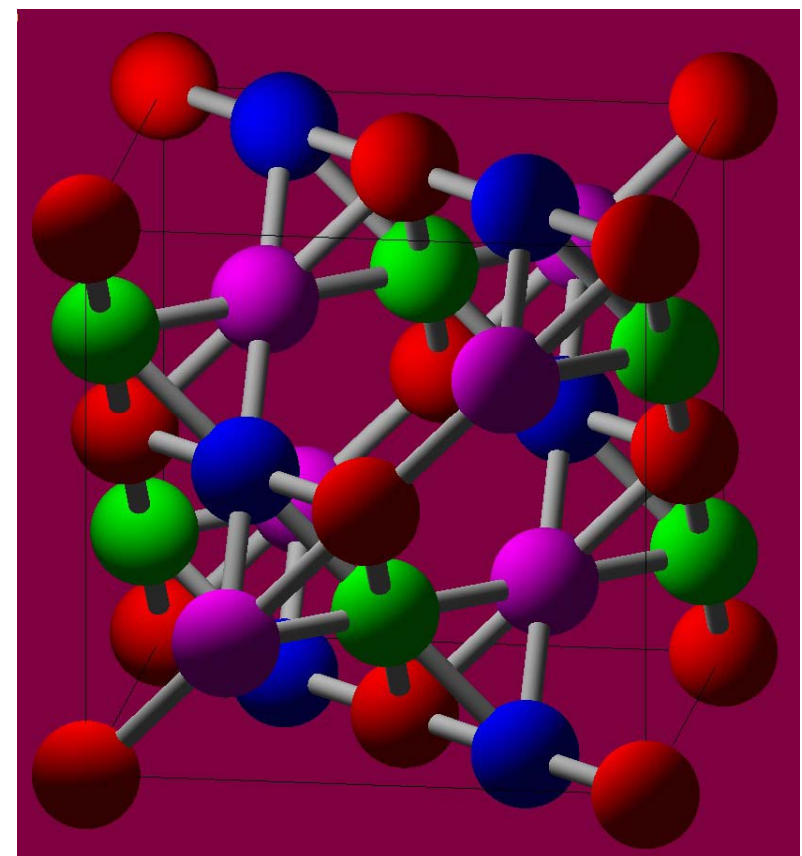
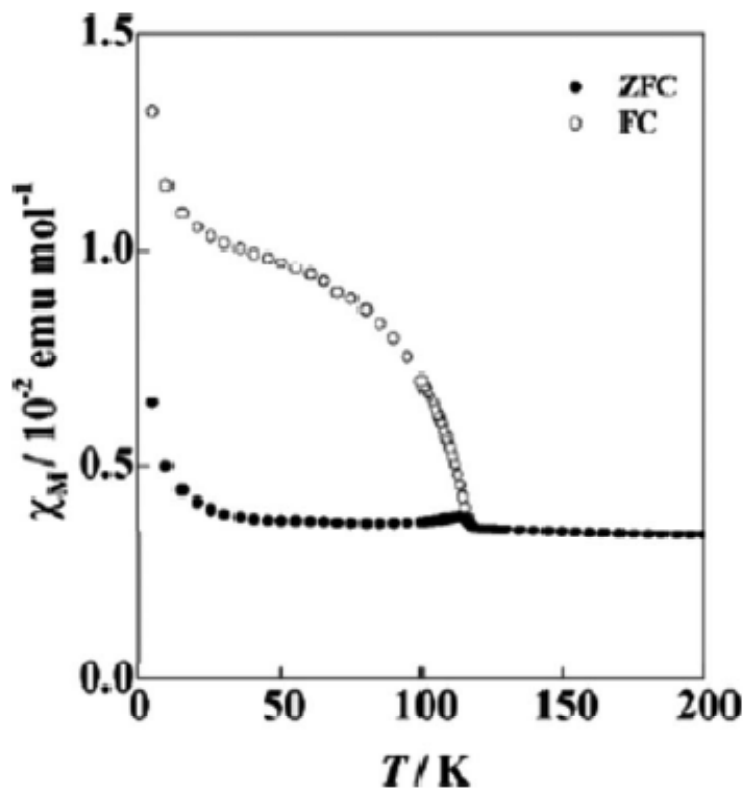


烧绿石结构 $A_2\text{Ir}_2\text{O}_7$

这些材料表现强的磁响应

实验定磁结构不容易

基本没有能带计算的工作



Magnetic susceptibility for $\text{Sm}_2\text{Ir}_2\text{O}_7$

烧绿石结构氧化物是强拓扑绝缘体？

ARTICLES

PUBLISHED ONLINE: 21 MARCH 2010 | DOI: 10.1038/NPHYS1606

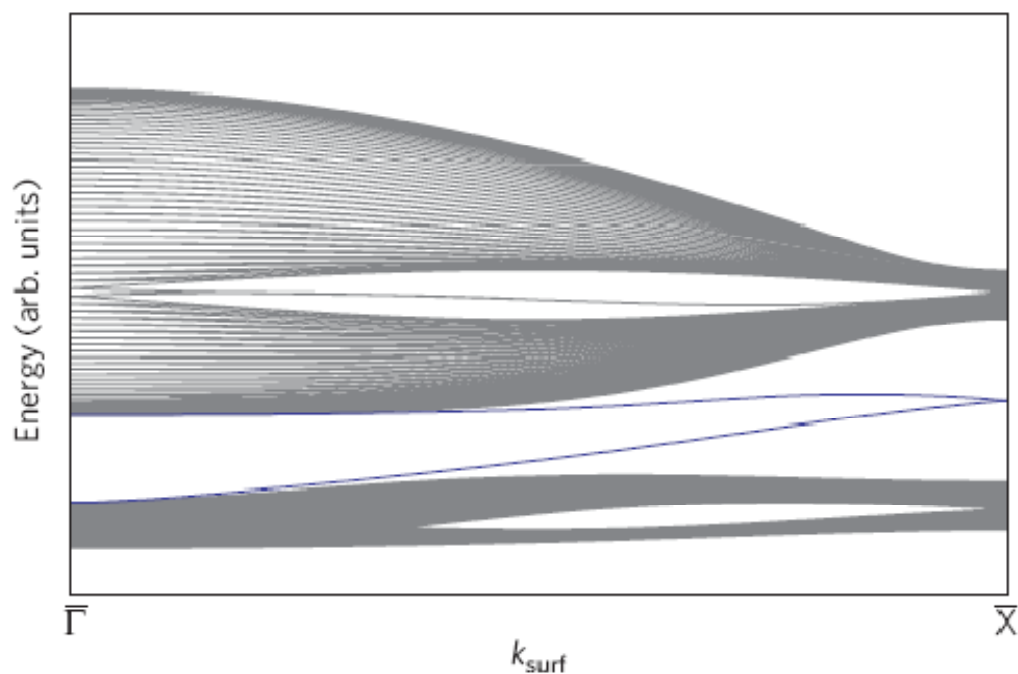
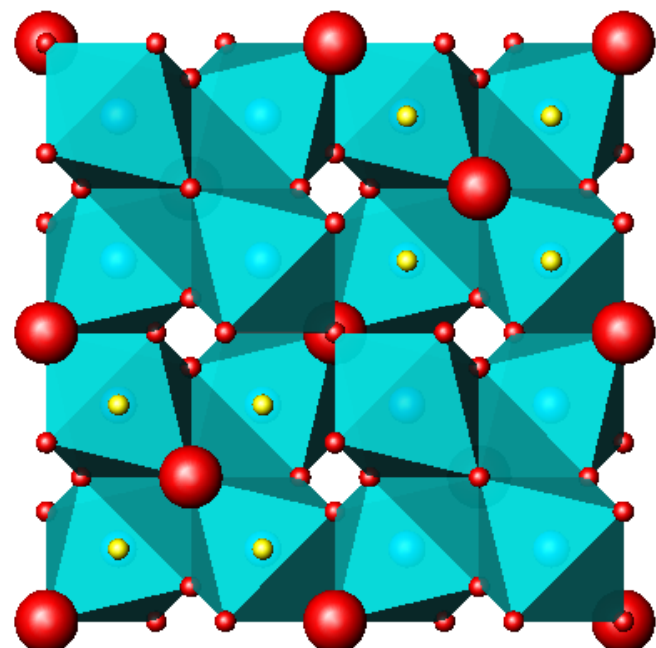
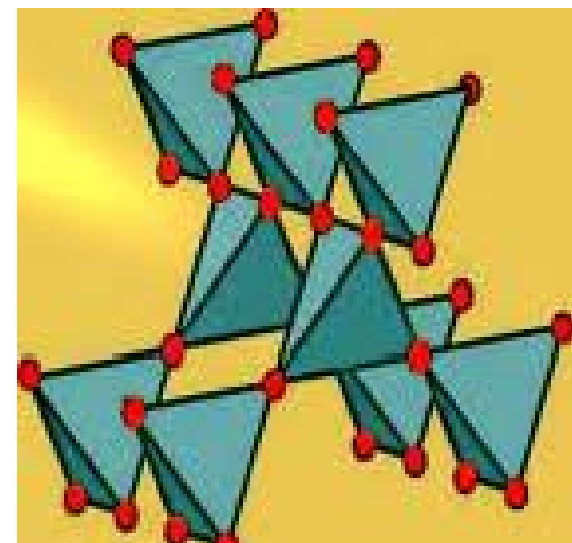
nature
physics

Mott physics and band topology in materials with strong spin-orbit interaction



Dmytro Pesin^{1,2*} and Leon Balents²

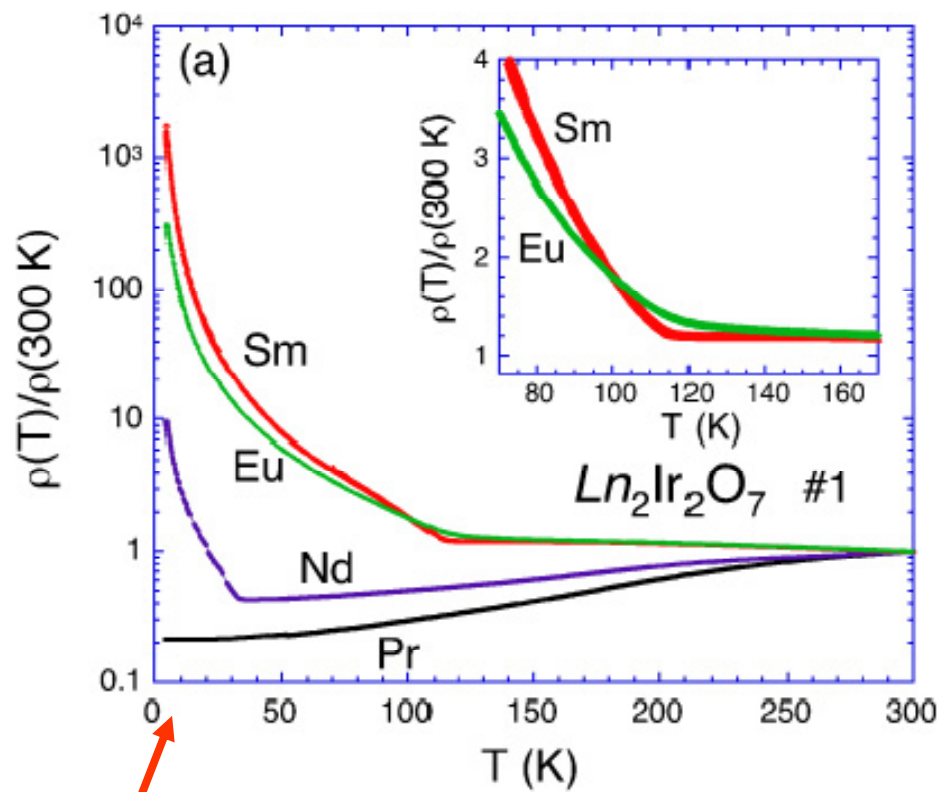
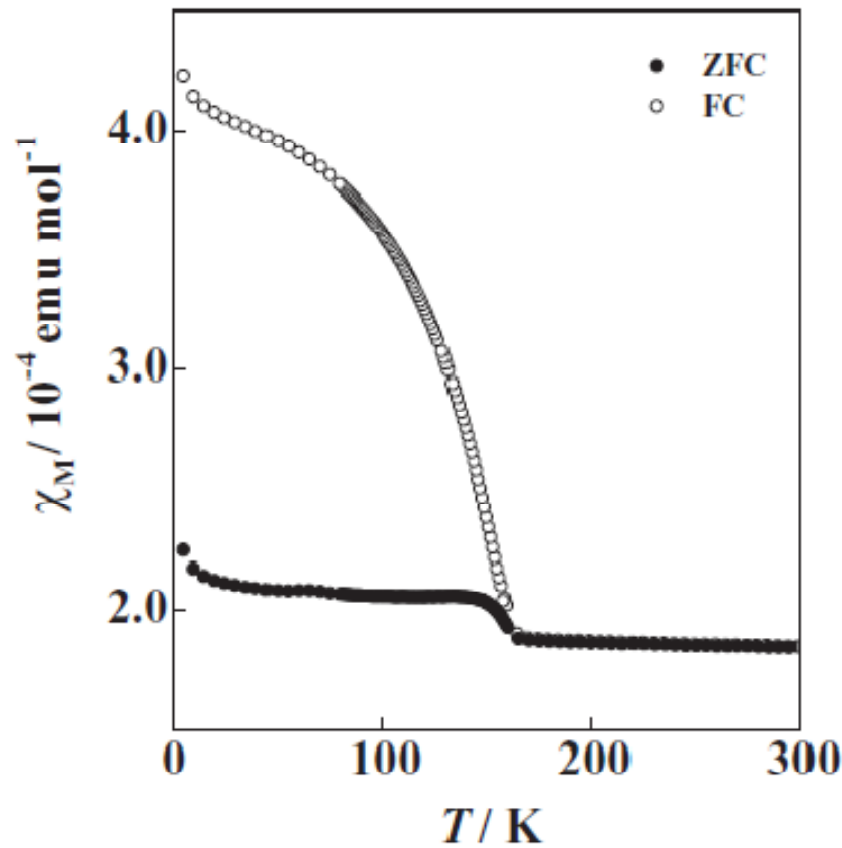
Recent theory and experiment have revealed that strong spin-orbit coupling can have marked qualitative effects on the band structure of weakly interacting solids, leading to a distinct phase of matter, the topological band insulator. We show that spin-orbit interaction also has quantitative and qualitative effects on the correlation-driven Mott insulator transition. Taking Ir-based pyrochlores as a specific example, we predict that for weak electron-electron interaction Ir electrons are in metallic and topological band insulator phases at weak and strong spin-orbit interaction, respectively. We show that by increasing the electron-electron interaction strength, the effects of spin-orbit coupling are enhanced. With increasing interactions, the topological band insulator is transformed into a ‘topological Mott insulator’ phase having gapless surface spin-only excitations. The proposed phase diagram also includes a region of gapless Mott insulator with a spinon Fermi surface, and a magnetically ordered state at still larger electron-electron interaction.



内容

- 5d过渡金属氧化物
- 烧绿石结构铱化合物
- 磁基态构型,Weyl半金属,Fermi Arc
- 设计Axion绝缘体

烧绿石结构铱氧化物 $A_2\text{Ir}_2\text{O}_7$ (A=Y,稀土元素) 实验事实

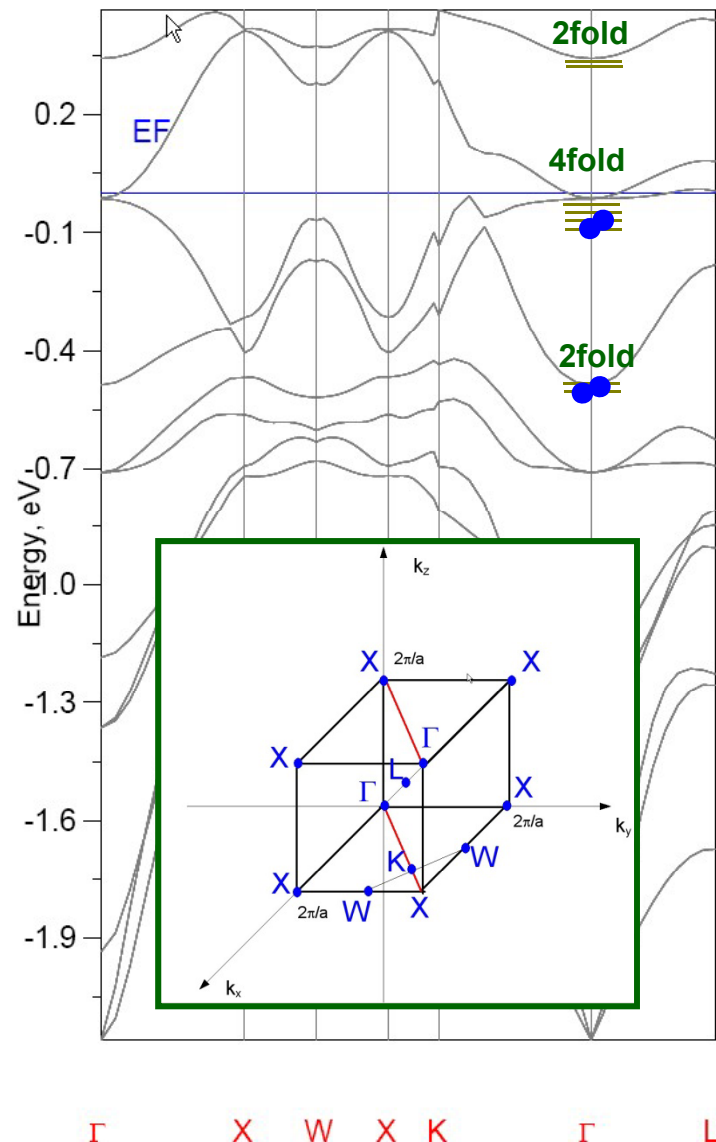


MATSUHIRA et al., (2007)

U !!!

N. Taira, M. Wakushima and Y. Hinatsu
(2001)

局域密度近似+自旋轨道耦合计算



Fermi Level

- $\text{Y}_2\text{Ir}_2\text{O}_7$ 元胞里面有4个Ir原子，所以有8个相对论的 $|\Gamma_7\rangle$ 态
- 每个Ir的 $|\Gamma_7\rangle$ 带填一个电子(每个 $J=3/2$ 带填4个电子，成为满带); 所以总的 $|\text{G}7\rangle$ 带填4个电子.
- 在 Γ 点的简并度为**2-4-2**. 填4个电子→metal!

几何阻错结构磁性基态的找寻

$$J_{\tau R \tau' R'}^{\alpha\beta} = \sum_{\mathbf{q}} \sum_{\mathbf{k} j j'} \frac{f_{\mathbf{k} j} - f_{\mathbf{k} + \mathbf{q} j'}}{\epsilon_{\mathbf{k} j} - \epsilon_{\mathbf{k} + \mathbf{q} j'}} \langle \psi_{\mathbf{k} j} | [\sigma \times \mathbf{B}_\tau]_\alpha | \psi_{\mathbf{k} + \mathbf{q} j'} \rangle \langle \psi_{\mathbf{k} + \mathbf{q} j'} | [\sigma \times \mathbf{B}_{\tau'}]_\beta | \psi_{\mathbf{k} j} \rangle e^{i \mathbf{q} (\mathbf{R} - \mathbf{R}')}$$

X. Wan, Q. Yin, S.Y. Savrasov, PRL 97, 266403

X. Wan, T. A. Maier, and S. Y. Savrasov, PRB 79, 155114

X. Wan, J. Dong, and S. Y. Savrasov, PRB 83, 205201

X. Wan, M. Kohno, and X. Hu, PRL 94, 087205

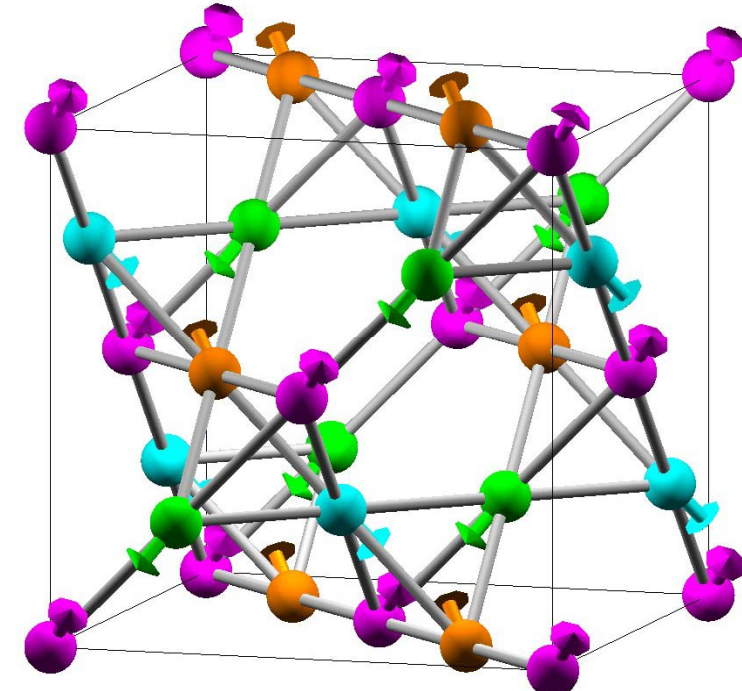
X. Wan, M. Kohno, and X. Hu, PRL 95, 146602

磁性基态构型

All-in/all-out非共线磁结构

- 根据:

- 1) 有转过去的趋势
- 2) 此构型是我们计算的唯一稳定的磁构型
- 3) $J(q)$ 在 $q=0$ 是极大
- 4) 没有Fermi surface nesting



实验证实

S

Magnetic transition, long-range order, and moment fluctuations in the pyrochlore iridate $\text{Eu}_2\text{Ir}_2\text{O}_7$

Songrui Zhao,^{1,*} J. M. Mackie,¹ D. E. MacLaughlin,¹ O. O. Bernal,² J. J. Ishikawa,³ Y. Ohta,³ and S. Nakatsuji³

Muon spin rotation and relaxation experiments in the pyrochlore iridate $\text{Eu}_2\text{Ir}_2\text{O}_7$ yield a well-defined muon spin precession frequency below the metal-insulator/antiferromagnetic transition temperature $T_M = 120$ K, indicative of long-range commensurate magnetic order and thus ruling out quantum spin liquid and spin-glass-like ground states. The dynamic muon spin relaxation rate is temperature-independent between 2 K and $\sim T_M$ and yields an

Magnetic order in the pyrochlore iridates $A_2\text{Ir}_2\text{O}_7$ ($A = \text{Y}, \text{Yb}$)

S. M. Disseler,¹ Chetan Dhital,¹ A. Amato,² S. R. Giblin,³ Clarina de la Cruz,⁴ Stephen D. Wilson,¹ and M. J. Graf^{1,*}

¹*Department of Physics, Boston College, Chestnut Hill, Massachusetts 02467, USA*

We present results from muon spin relaxation/rotation, magnetization, neutron scattering, and transport measurements on polycrystalline samples of the pyrochlore iridates $\text{Y}_2\text{Ir}_2\text{O}_7$ (Y-227) and $\text{Yb}_2\text{Ir}_2\text{O}_7$ (Yb-227). Well-defined spontaneous oscillations of the muon asymmetry are observed together with hysteretic behavior in magnetization below 130 K in Yb-227, indicative of commensurate long-range magnetic order. Similar

实验证实

Magnetic order and the electronic ground state in the pyrochlore iridate $\text{Nd}_2\text{Ir}_2\text{O}_7$

S. M. Disseler,¹ Chetan Dhital,¹ T. C. Hogan,¹ A. Amato,² S. R. Giblin,³ Clarina de la Cruz,⁴ A. Daoud-Aladine,³ Stephen D. Wilson,¹ and M. J. Graf¹

We report a muon spin relaxation/rotation, bulk magnetization, neutron scattering, and transport study of the electronic properties of $\text{Nd}_2\text{Ir}_2\text{O}_7$. We observe the onset of strongly hysteretic behavior in the temperature-dependent magnetization below 120 K, and an abrupt increase in the temperature-dependent resistivity below 8 K. Muon spin relaxation measurements show that the hysteretic magnetization is driven by a transition to a magnetically disordered state, and below 8 K a magnetically ordered ground state sets in, as evidenced by the onset of spontaneous muon precession. Our measurements point toward the absence of a true metal-to-insulator

Continuous transition between antiferromagnetic insulator and paramagnetic metal in the pyrochlore iridate $\text{Eu}_2\text{Ir}_2\text{O}_7$

Jun J. Ishikawa,* Eoin C. T. O’Farrell, and Satoru Nakatsuji[†]

Our single crystal study of the magnetothermal and transport properties of the pyrochlore iridate $\text{Eu}_2\text{Ir}_2\text{O}_7$ reveals a continuous phase transition from a paramagnetic metal to an antiferromagnetic insulator for a sample with stoichiometry within $\sim 1\%$ resolution. The insulating phase has strong proximity to an antiferromagnetic semimetal, which is stabilized by several % level of the off-stoichiometry. Our observations suggest that in addition to electronic correlation and spin-orbit coupling the magnetic order is essential for opening the charge gap.

实验证实

Emergence of Magnetic Long-range Order in Frustrated Pyrochlore $\text{Nd}_2\text{Ir}_2\text{O}_7$ with Metal-insulator Transition

K. Tomiyasu,^{1,*} K. Matsuhira,² K. Iwasa,¹ M. Watahiki,¹ S. Takagi,² M. Wakeshima,³ Y. Hinatsu,³ M. Yokoyama,⁴ K. Ohoyama,⁵ and K. Yamada⁶

In this study, we performed powder neutron diffraction and inelastic scattering measurements of frustrated pyrochlore $\text{Nd}_2\text{Ir}_2\text{O}_7$, which exhibits a metal-insulator transition at a temperature T_{MI} of 33 K. The diffraction measurements revealed that the pyrochlore has an antiferromagnetic long-range structure with propagation vector \mathbf{q}_0 of (0,0,0) and that it grows with decreasing temperature below 15 K. This structure was analyzed to be of the all-in all-out type, consisting of highly anisotropic Nd^{3+} magnetic moments of magnitude $2.3 \pm 0.4\mu_B$, where μ_B is the Bohr magneton. The inelastic scattering measurements revealed that the Kramers ground doublet of Nd^{3+} splits below T_{MI} . This suggests the appearance of a static internal magnetic field at the Nd sites, which probably originates from a magnetic order consisting of Ir^{4+} magnetic moments. Here, we discuss a magnetic structure model for the Ir order and the relation of the order to the metal-insulator transition in terms of frustration.

理论方面

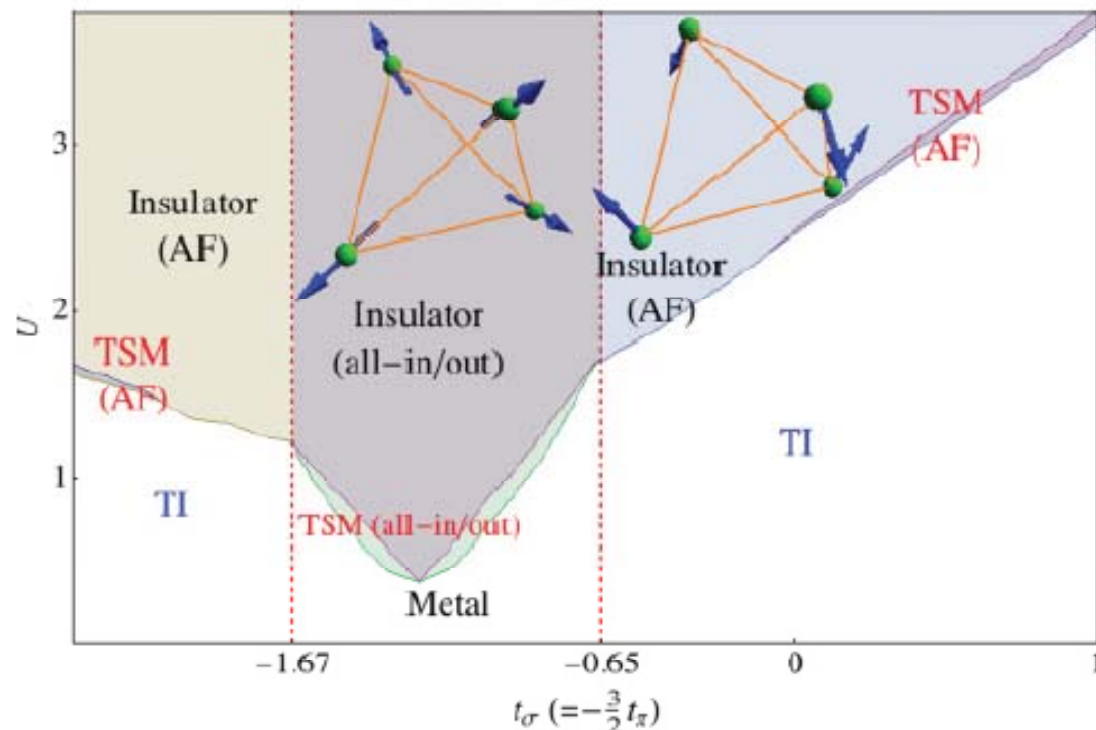
PHYSICAL REVIEW B 85, 045124 (2012)

Topological and magnetic phases of interacting electrons in the pyrochlore iridates

William Witczak-Krempa¹ and Yong Baek Kim^{1,2}

Mean field approximation

DCA

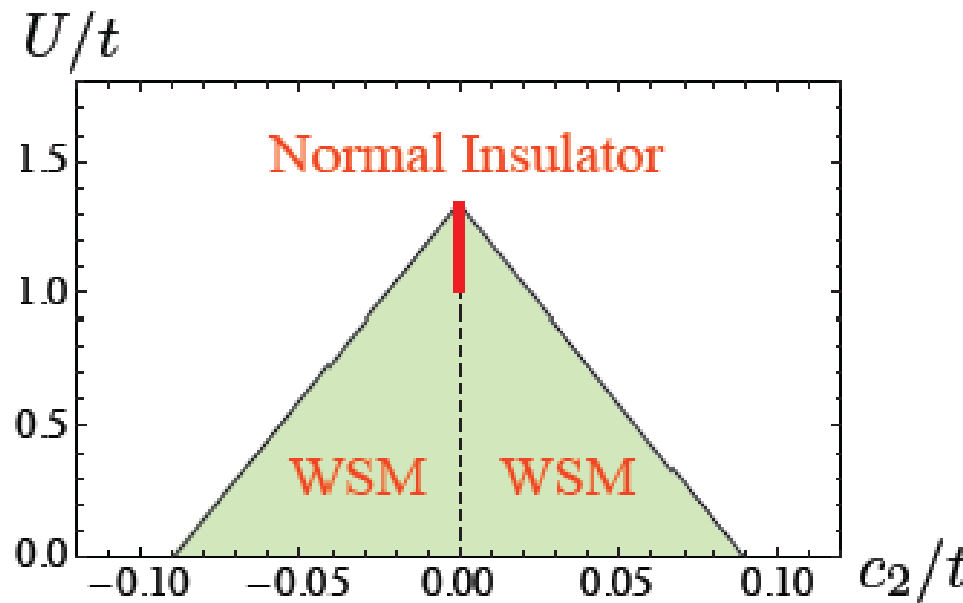


理论方面

Magnetic orders and topological phases from *f-d* exchange in pyrochlore iridates

Gang Chen and Michael Hermele

We study theoretically the effects of *f-d* magnetic exchange interaction in the $R_2Ir_2O_7$ pyrochlore iridates. The R^{3+} *f*-electrons form localized magnetic doublets due to the crystal field environment, while the Ir^{4+} *d*-electrons are more itinerant and feel a strong spin-orbit coupling. We construct and analyze a minimal model capturing this physics, treating the Ir subsystem using a Hubbard-type model. First neglecting the Hubbard interaction, we find Weyl semi-metal and Axion insulator phases induced by the *f-d* exchange. Next, we find that *f-d* exchange can cooperate with the Hubbard interaction to stabilize the Weyl semi-metal over a larger region of parameter space than when it is induced by *d*-electron correlations alone. Applications to experiments are discussed.



All-in/all-out非共线磁结构



PHYSICAL REVIEW B, VOLUME 63, 195104

2001

Continuous metal-insulator transition in the pyrochlore $\text{Cd}_2\text{Os}_2\text{O}_7$

D. Mandrus,^{1,2,*} J. R. Thompson,^{2,1} R. Gaal,³ L. Forro,³ J. C. Bryan,⁴ B. C. Chakoumakos,¹ L. M. Woods,^{2,1} B. C. Sales,¹ R. S. Fishman,¹ and V. Keppens^{1,†}

PHYSICAL REVIEW B, VOLUME 65, 155109

2002

Electronic structure of the pyrochlore metals $\text{Cd}_2\text{Os}_2\text{O}_7$ and $\text{Cd}_2\text{Re}_2\text{O}_7$

D. J. Singh

Code 6391, Naval Research Laboratory, Washington, DC 20375

P. Blaha and K. Schwarz

Institut für Physik und Theoretische Chemie, TU Wien, A-1060 Wien, Austria

J. O. Sofo

All-in/all-out非共线磁结构

PRL 108, 247204 (2012)

PHYSICAL REVIEW LETTERS

week ending
15 JUNE 2012

Noncollinear Magnetism and Spin-Orbit Coupling in 5d Pyrochlore Oxide $\text{Cd}_2\text{Os}_2\text{O}_7$

We investigate the electronic and magnetic properties of the pyrochlore oxide $\text{Cd}_2\text{Os}_2\text{O}_7$ using the density-functional theory plus on-site repulsion (U) method, and depict the ground-state phase diagram with respect to U . We conclude that the all-in-all-out noncollinear magnetic order is stable in a wide range of U . We also show that the easy-axis anisotropy arising from the spin-orbit coupling plays a significant role in stabilizing the all-in-all-out magnetic order. A *pseudogap* was observed near the transition between

PRL 108, 247205 (2012)

PHYSICAL REVIEW LETTERS

week ending
15 JUNE 2012

Tetrahedral Magnetic Order and the Metal-Insulator Transition in the Pyrochlore Lattice of $\text{Cd}_2\text{Os}_2\text{O}_7$

accompanied with any spatial symmetry breaking. We propose a noncollinear all-in-all-out spin arrangement on the tetrahedral network made of Os atoms. Based on this we suggest that the transition is not caused by the Slater mechanism as believed earlier but by an alternative mechanism related to the

内容

- 5d过渡金属氧化物
- 烧绿石结构铱化合物
- 磁基态构型, Weyl半金属, Fermi Arc
- 设计Axion绝缘体

电子关联+自旋轨道耦合→新的物理？

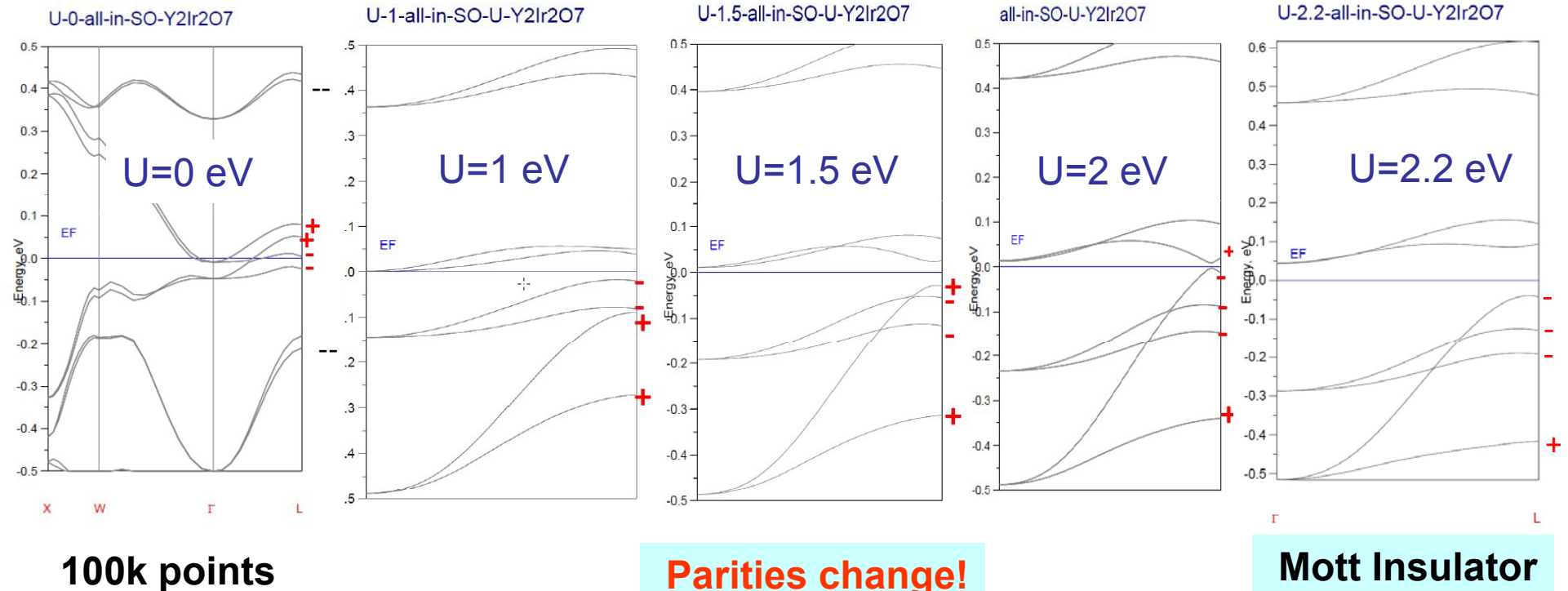
这里是磁性打破了时间反演，所以这个体系不是
常规的拓扑绝缘体。

是否有新的物理？

绝缘体 只要能隙没有闭合，其拓扑量子序不变。
所以对于绝缘体可以定义拓扑性质。

对于金属呢？

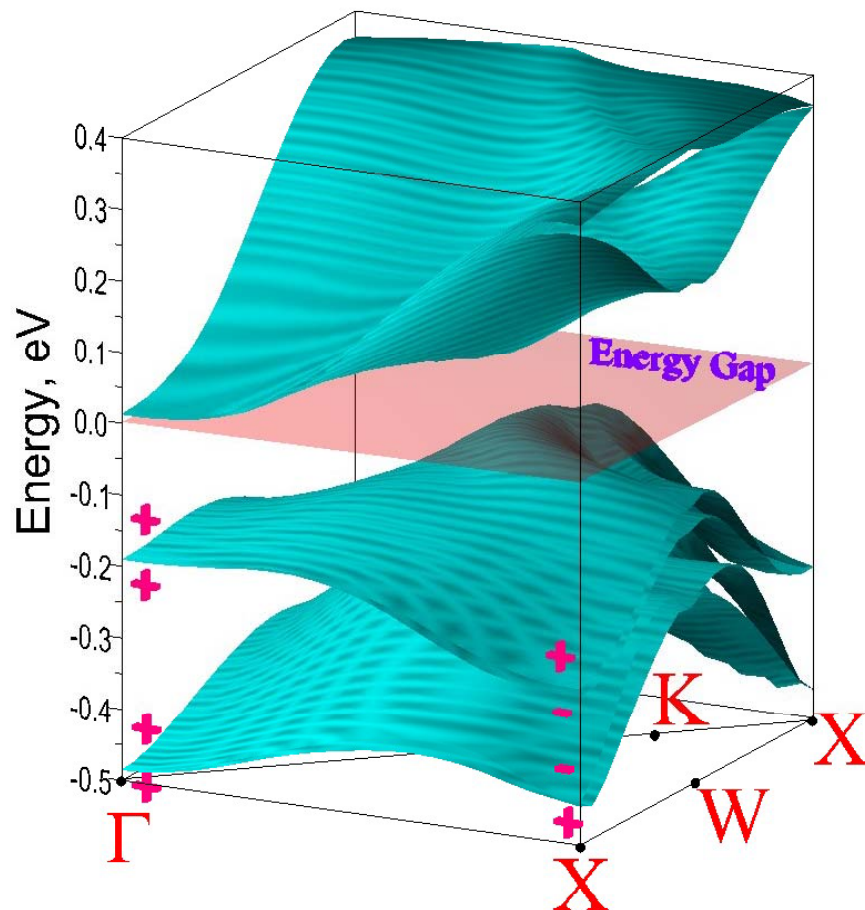
反常的能带行为 宇称反转



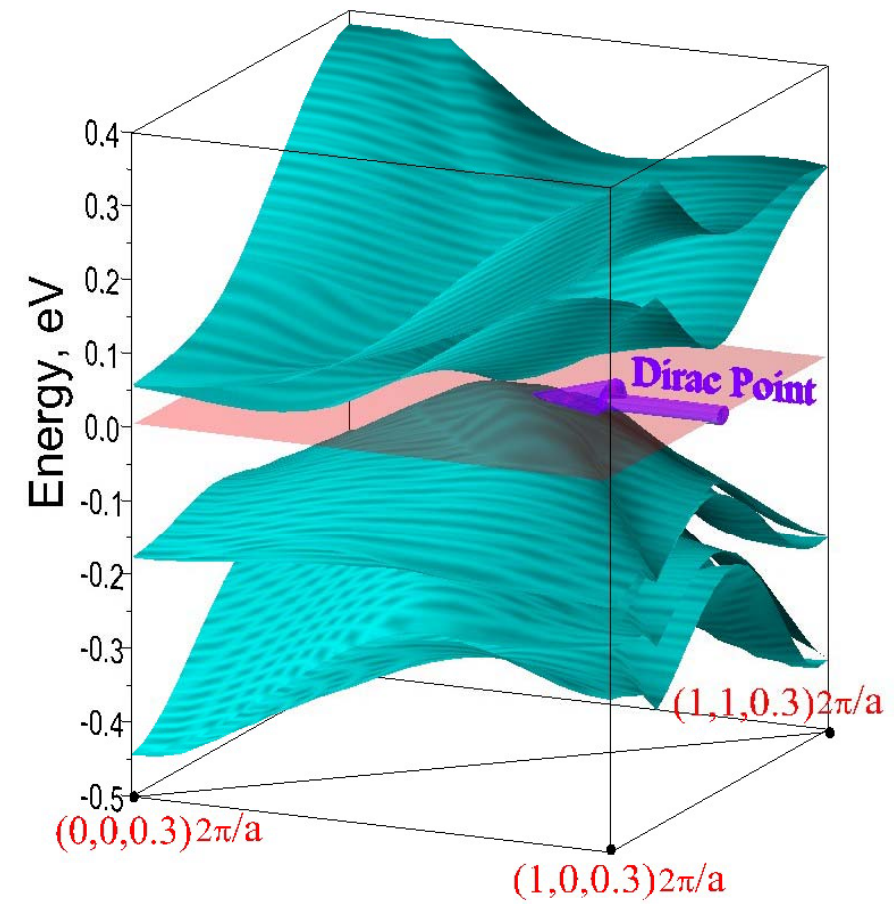
We study changes in band parities that may indicate a presence of topological insulator and also semi-metallic phase since topological insulators in 3D must be separated from trivial insulator by 3D Dirac (Weyl) points (Murakami, Kuga, 2008).

在合理的U的范围内 ($1.0\text{eV} < U < 1.8 \text{ eV}$) 是Weyl semi-metal

LEFT:within $k_z=0$ plane of BZ



RIGHT:for $k_z=0.3$ plane of BZ



Arita et al., PRL (2012) → U在 $1.4 \rightarrow 2.3 \text{ eV}$

Weyl-semimetal

- Graphene 里面的Dirac point 是4分量的)。
- Weyl点一旦产生，就非常稳定，小的扰动不能把它消灭。只有2个具有相反符号的Weyl点相遇，Weyl点才能消失，材料变为绝缘体。
- 要打破时间反演或空间反演不变。

$$\begin{pmatrix} A & C \\ C^* & B \end{pmatrix} \circledast \begin{pmatrix} A & \blacksquare & B \\ \text{Re } C & \blacksquare & 0 \\ \text{Im } C & \blacksquare & 0 \end{pmatrix}, \quad k_x, k_y, k_z$$

金属 拓扑？

- 绝缘体 只要能隙没有闭合，其拓扑量子序不变。所以对于绝缘体可以定义拓扑性质。
- 对于金属呢？

Weyl-semimetal

In the vicinity of Weyl Point: $q = k - k_W$

$$H(q) = \sum_{i=x,y,z} v_i \bullet q \sigma_i \quad E_{\pm}(q) = \pm \sqrt{\sum_{i=x,y,z} (v_i \bullet q)^2}$$

The Berry curvature is evaluated to be

$$\Omega(k) = i \sum_{n=1}^{N_{occ}} \langle \nabla_k u_{kn} | \times | \nabla_k u_{kn} \rangle \rightarrow \sum_{ijk} \frac{1}{2} \epsilon_{ijk} (v_i \times v_j) (v_k \bullet q) \frac{1}{\left(\sum_i (v_i \bullet q)^2 \right)^{3/2}}$$

Integrating over small sphere surrounding Weyl point produces flux that is given by chiral charge c

$$c = \frac{1}{2\pi} \oint_S dS \Omega(k) = \text{sign}(v_1 \bullet v_2 \times v_3)$$

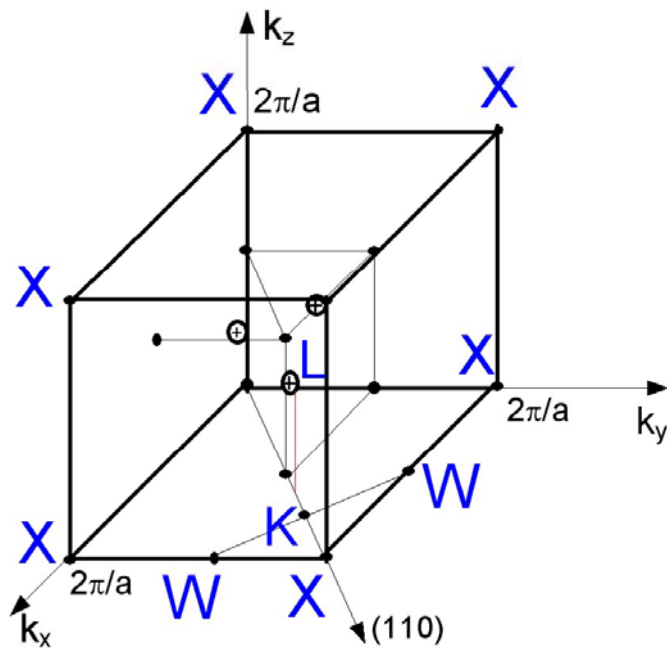
Weyl point acts as a magnetic monopole at the origin:

$$\Omega(q) = c \frac{1}{2} \frac{q}{q^3}$$

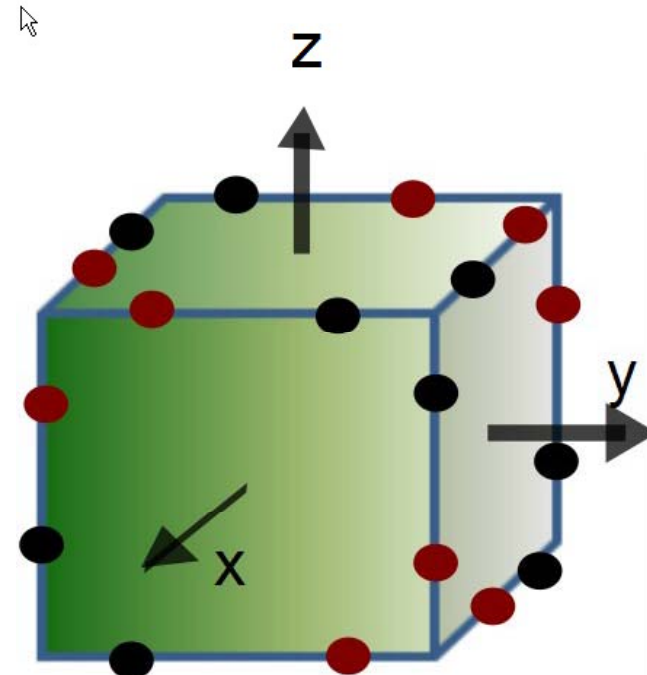
“点电荷”

Charge determined in terms of electron velocities at this k_D point:

$$c = \text{sign}(\nu_1 \bullet \nu_2 \times \nu_3)$$



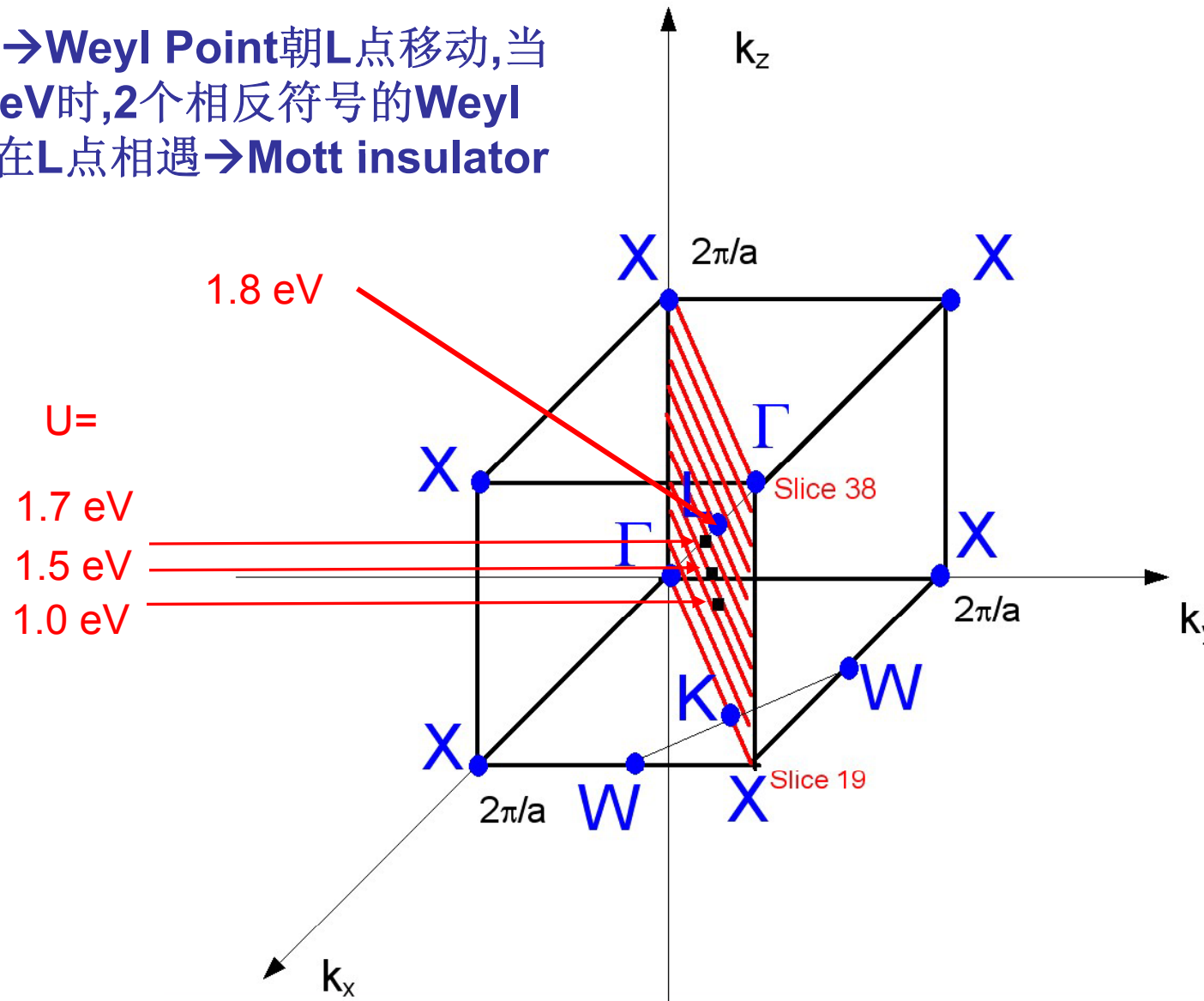
Three positive Weyl points around L



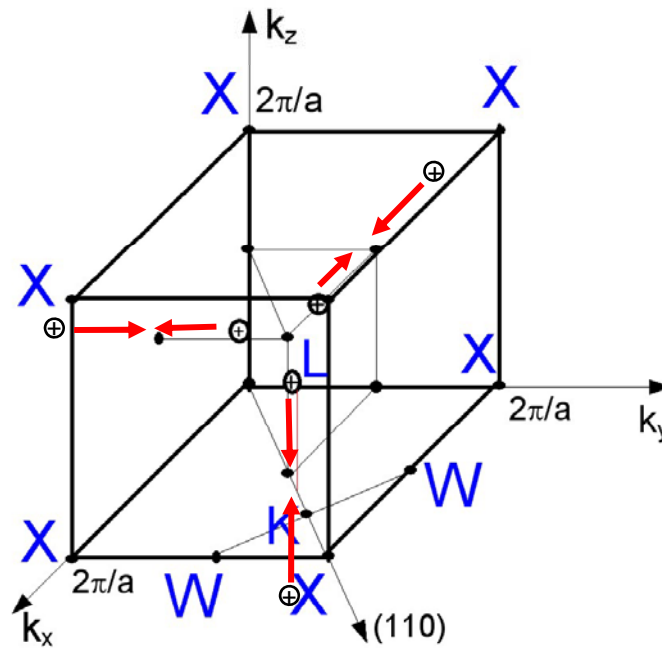
Positive and negative Weyl points in BZ

变化U的影响

增加 $U \rightarrow$ Weyl Point 朝 L 点移动, 当
 $U=1.8\text{ eV}$ 时, 2个相反符号的 Weyl
Point 在 L 点相遇 \rightarrow Mott insulator



变化U的影响

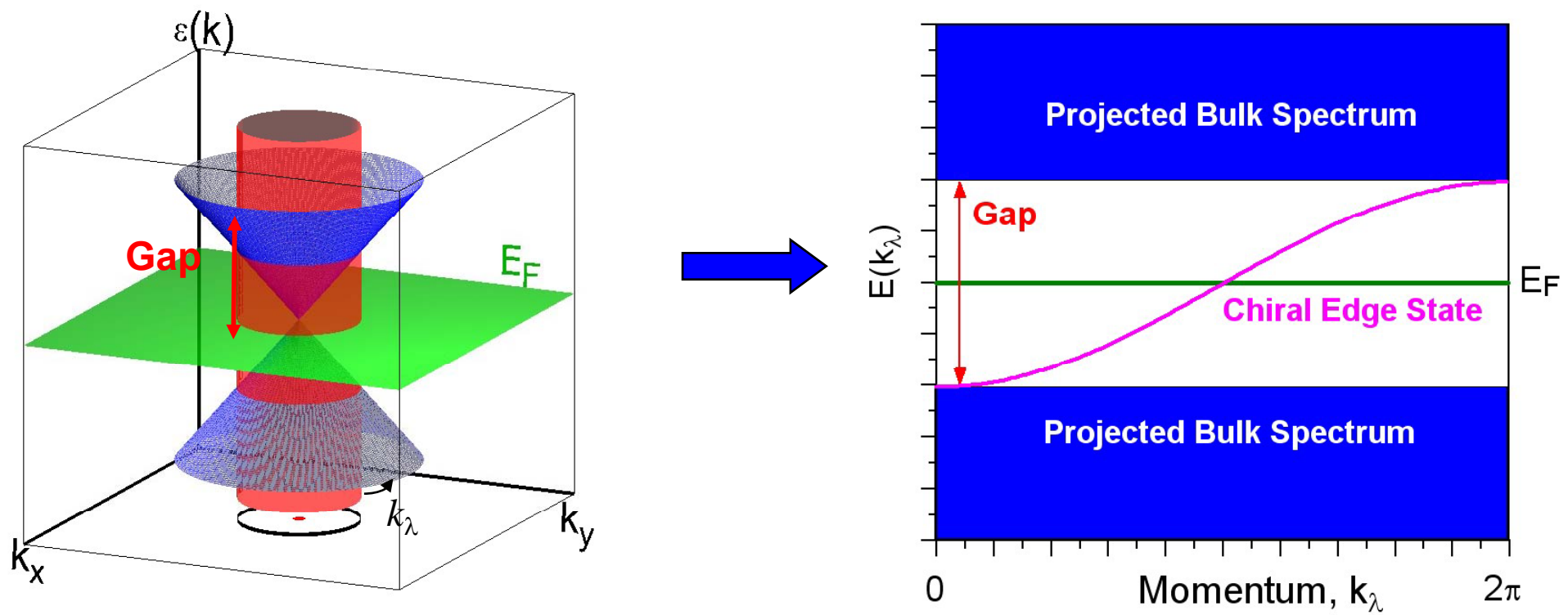


减小U→Weyl Point朝X点移动,当U=1.0eV时,2个相反符号的Weyl Point在X点相遇.如果材料是绝缘体的话将是Axion Insulator
但是LDA+SO+U发现别处有能带通过Fermi level

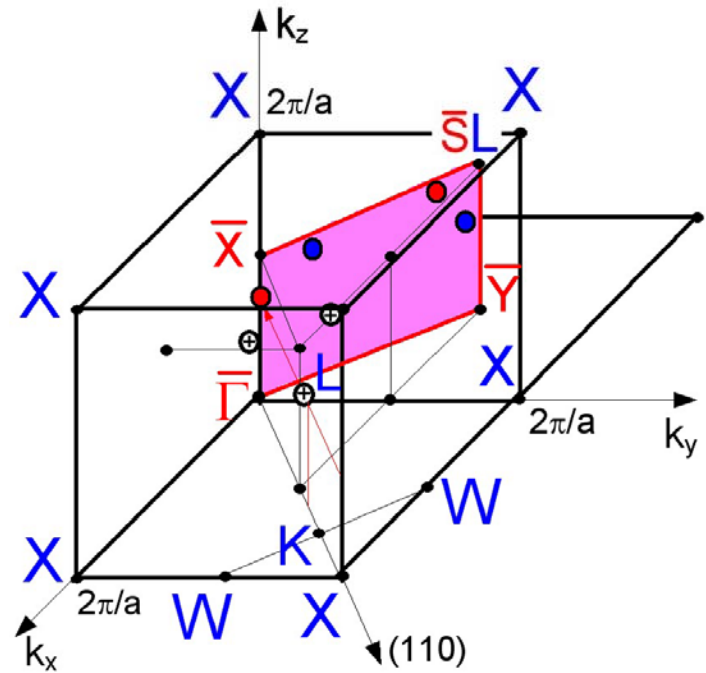
内容

- 5d过渡金属氧化物
- 烧绿石结构铱化合物
- 磁基态构型, Weyl半金属, Fermi Arc
- 设计Axion绝缘体

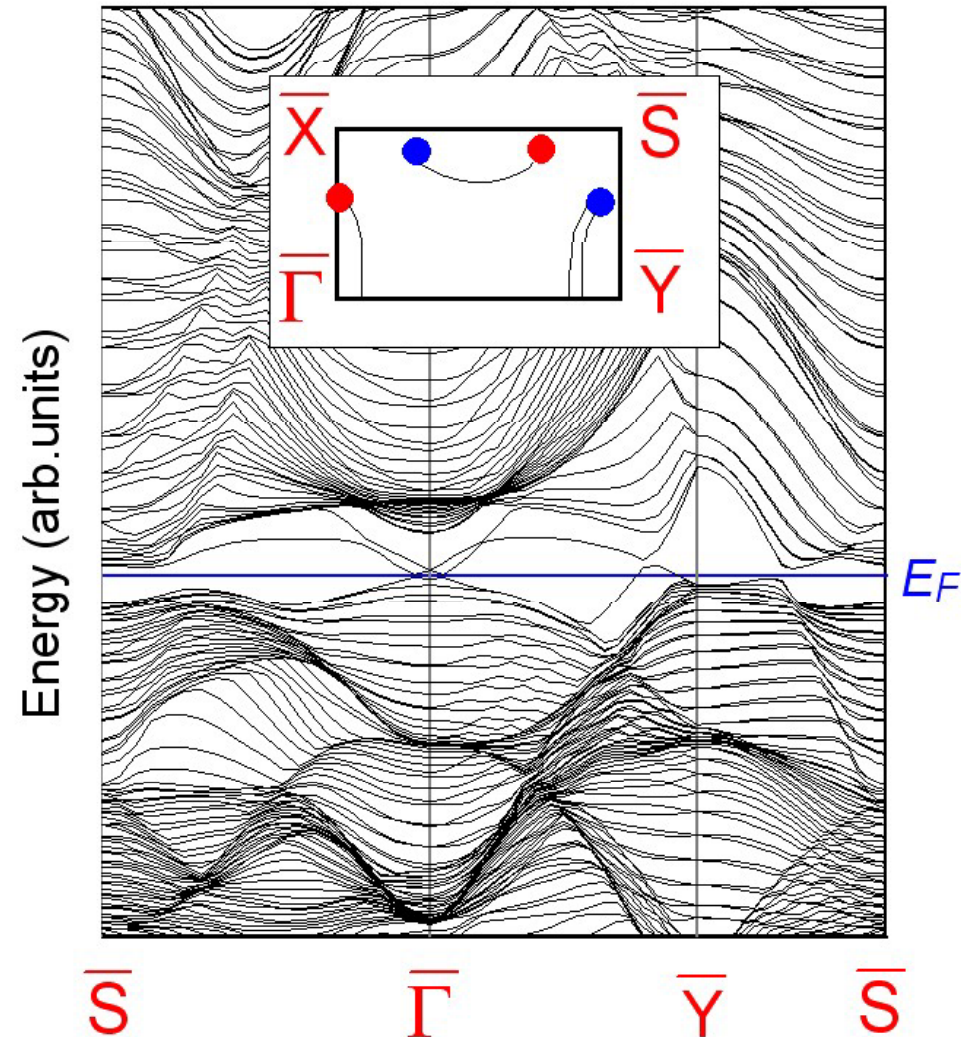
Fermi Arc (费米面是不连续的线段)



Fermi Arc (topo→费米面是不连续的线段)

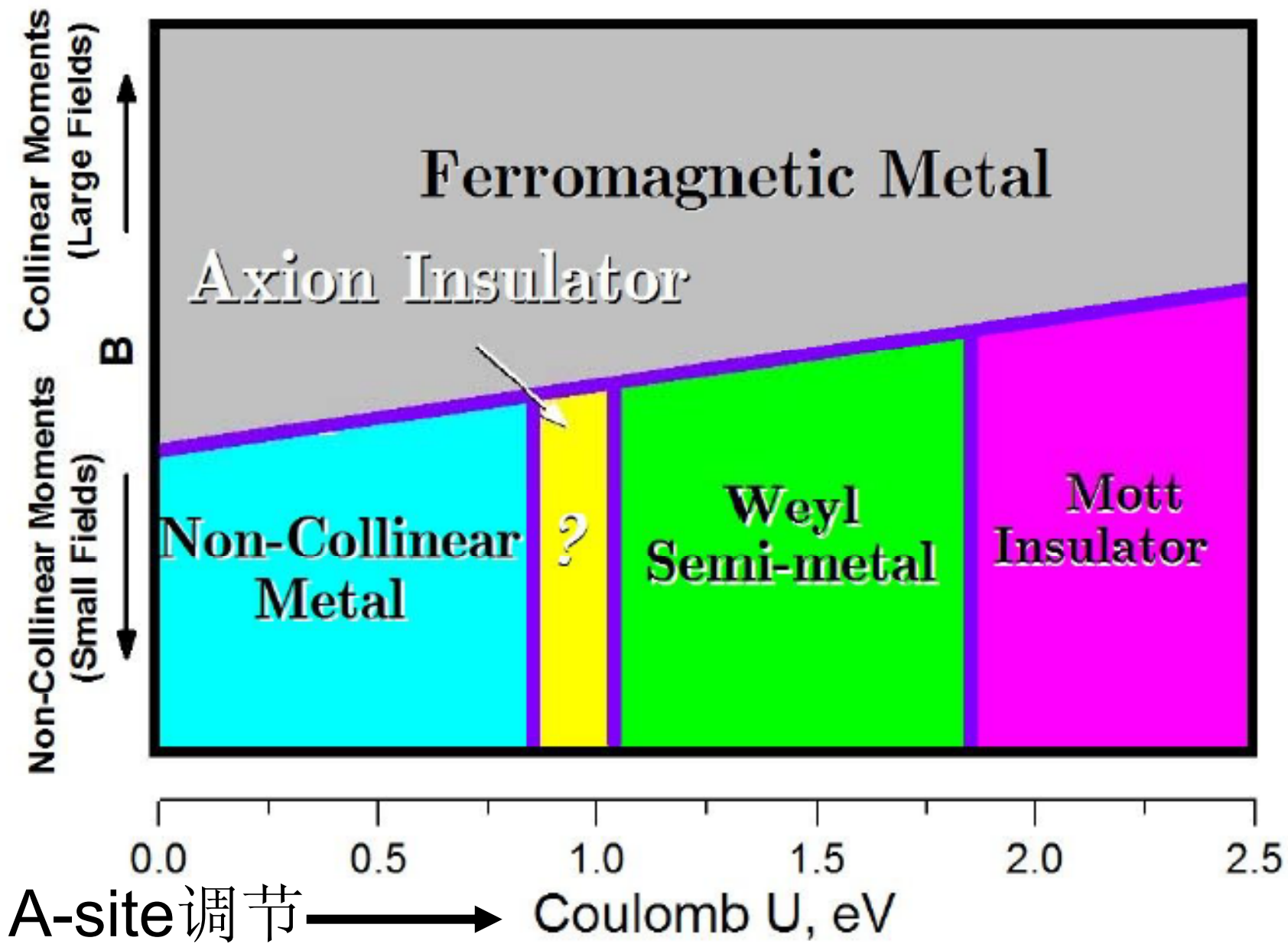


(110) 面



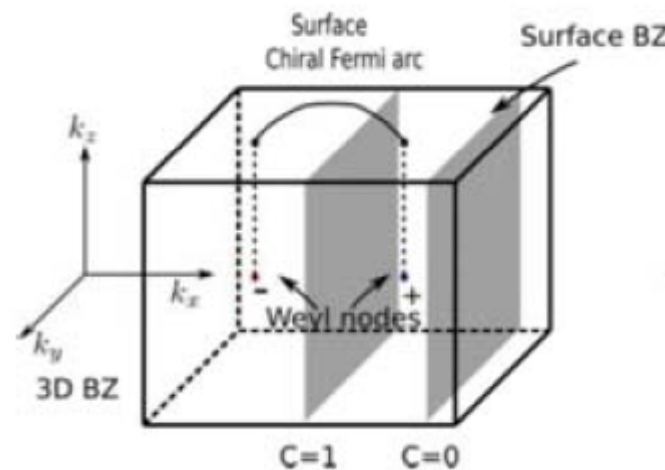
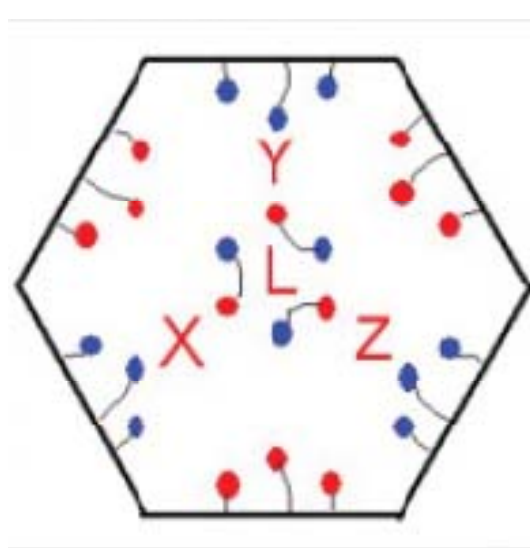
Fermi Arcs connecting Weyl points of opposite chirality can be directly observed

烧绿石结构Ir氧化物 ($A_2Ir_2O_7$) 相图



新型的拓扑量子态—Weyl半金属

- a) Weyl点是稳定的
- b) 有受拓扑保护的表面态，即非闭合的费米面(Fermi arc)
- c) 它对外场的响应也由其拓扑性质决定(只与Weyl点的位置有关，和能带的细节无关)。



相关实验

PRL 109, 136402 (2012)

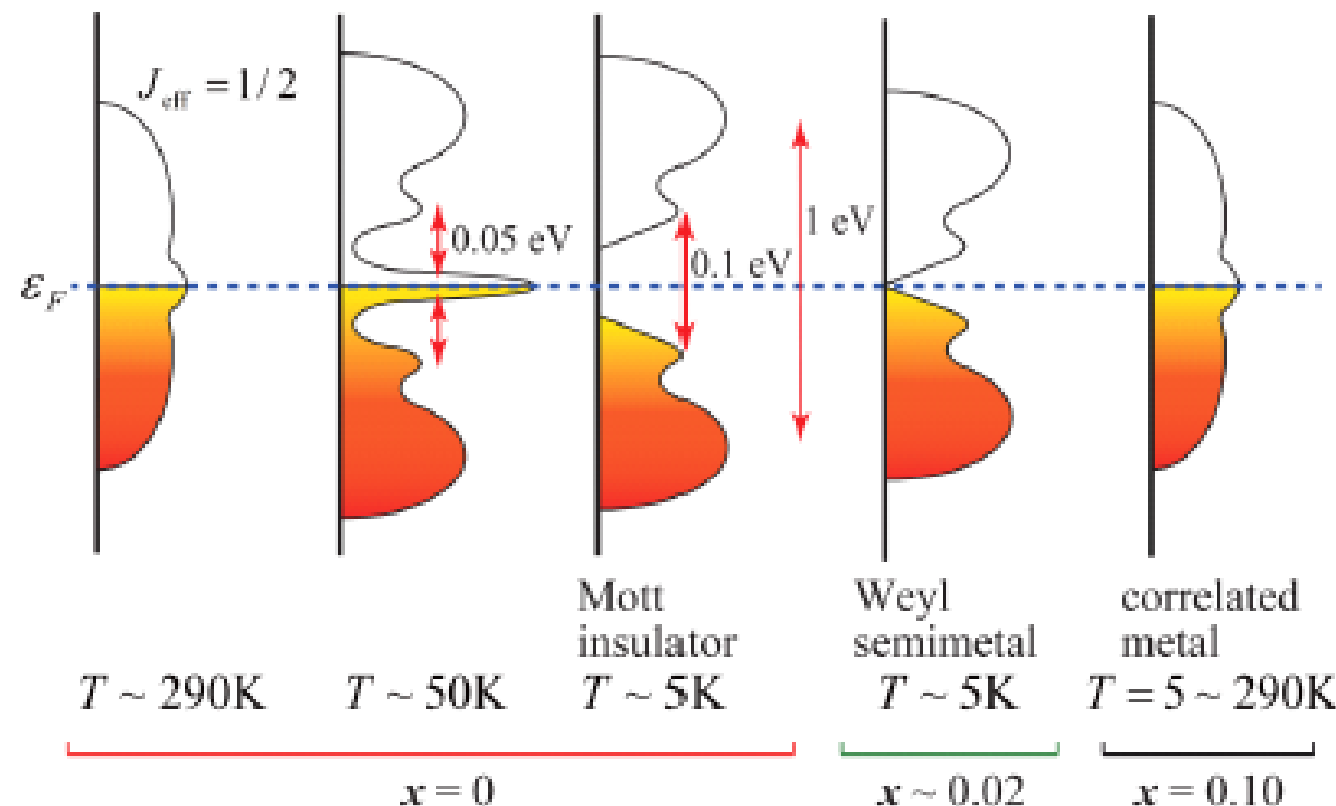
PHYSICAL REVIEW LETTERS

WE
28 SEP

Variation of Charge Dynamics in the Course of Metal-Insulator Transition for Pyrochlore-Type $\text{Nd}_2\text{Ir}_2\text{O}_7$

K. Ueda,¹ J. Fujioka,¹ Y. Takahashi,¹ T. Suzuki,² S. Ishiwata,¹ Y. Taguchi,² and Y. Tokura^{1,2}

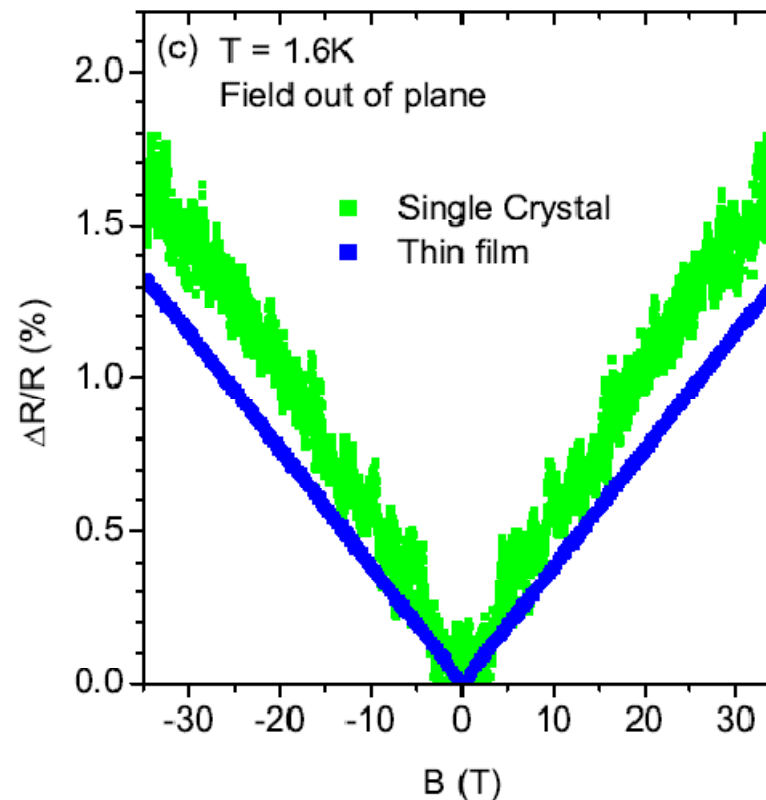
(c)



相关实验

Linear magnetoresistance and time reversal symmetry breaking of pyrochlore iridates
 $\text{Bi}_2\text{Ir}_2\text{O}_7$

Jiun-Haw Chu,^{1, 2,*} Scott. C. Riggs,^{3, 4} Maxwell Shapiro,^{3, 4} Jian Liu,^{1, 2} Claudio Ryan Serero,⁵ Di Yi,⁵ M. Melissa,¹ S. J. Suresha,² C. Frontera,⁶ Ashvin Vishwanath,^{1, 2} Xavi Marti,⁵ I. R. Fisher,^{3, 4} and R. Ramesh^{1, 5, 2}



内容

- 5d过渡金属氧化物
- 烧绿石结构铱化合物

磁基态构型,Weyl半金属,Fermi Arc

- 设计Axion绝缘体

Axion Insulators

ARTICLES

PUBLISHED ONLINE: 7 MARCH 2010 | DOI:10.1038/NPHYS1534

nature
physics

Dynamical axion field in topological magnetic insulators

Rundong Li¹, Jing Wang^{1,2}, Xiao-Liang Qi¹ and Shou-Cheng Zhang^{1*}

$$S_0 = \frac{8}{\pi} \int d^3x dt \left(\varepsilon E^2 - B^2 / \mu \right)$$

$$S_\theta = \frac{\theta}{2\pi} \frac{e^2}{2\pi\hbar c} \int d^3x dt \vec{E} \cdot \vec{B}$$

时间反演对称 $\rightarrow \Theta=0, \pi$

空间反演对称 $\rightarrow \Theta=0, \pi$

没有时间空间反演对称 $\rightarrow \Theta$ 不再量子化，但是都很小 $BFO, 10^{-4}$

磁+拓扑

- The simplest way is to coat a topological insulator with magnetic material to get rid of surface states. that will also have $\theta = \pi$, but there are technical problems there. (Y.L. Chen et al., Science (2010))
- Combine band topology with intrinsic magnetic order.

设计大的磁电响应材料

- 磁需要电子关联
- 拓扑量子序需要自旋轨道耦合
- Bi_2Se_3 等已知的不好
- 3d,4d不好
- 4f,5f不好
- **5d !**

计算 θ

Turner, Zhang, Vishwanath, arXiv:1010.4335
Hughes, Prodan and Bernevig, PRB (2011)

$$P \quad \blacksquare \quad \bullet \frac{e^2}{2\mathcal{W}} B$$

$$\theta = \pi \cdot M(\bmod \ 2)$$

where $M = (\sum_k N_i)/2$, and N_i is the number of occupied states at the TRIM points i with odd parity.

TABLE III: Calculated parities of states at Time Reversal Invariant Momenta (TRIMs) of CaOs_2O_4 . Only the 4 empty t_{2g} bands are shown in order of increasing energy. $\text{Lx } 2\pi/a(-0.5, 0.5, 0.5)$, $\text{Ly } 2\pi/a(0.5, -0.5, 0.5)$, $\text{Lz } 2\pi/a(-0.5, 0.5, 0.5)$ and $\text{L } 2\pi/a(0.5, 0.5, 0.5)$.

	Lx	Ly	Lz	L
$U=0.5 \text{ eV}$	++++	++++	+++	- - - -
$U=1.5 \text{ eV}$	-+++	-+++	-+++	+ - - -

CaOs_2O_4

SrOs_2O_4

PRL 108, 146601 (2012)

Xiangang Wan,¹ Ashvin Vishwanath,^{2,3} and Sergey Y. Savrasov⁴

设计Axion insulator

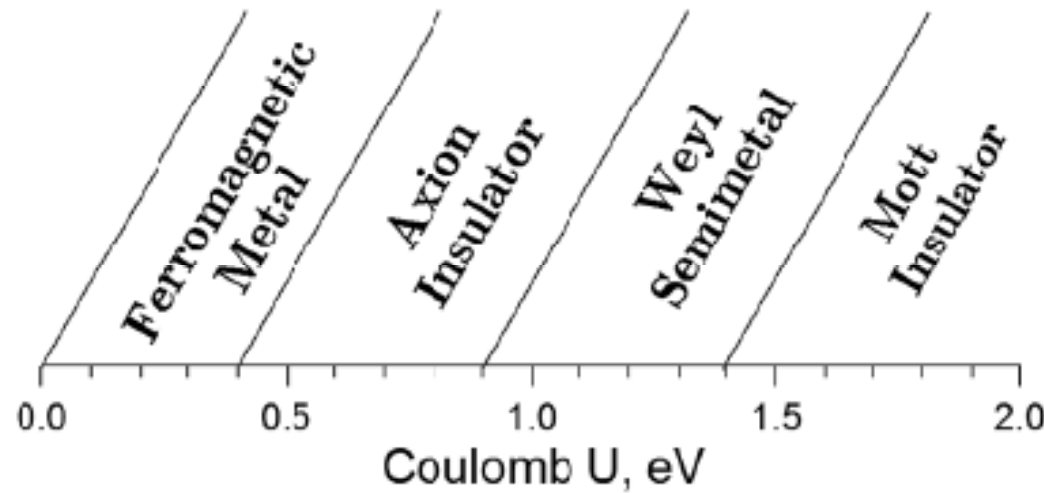


FIG. 3. Sketch of the predicted phase diagram for spinel osmulates.

PRL 108, 146601 (2012)

Xiangang Wan,¹ Ashvin Vishwanath,^{2,3} and Sergey Y. Savrasov⁴

汇报内容

- 5d过渡金属氧化物
- 烧绿石结构铱化合物
- 磁基态构型, Weyl半金属, Fermi Arc
- 设计Axion绝缘体
- Slater insulator

Slater Insulator

- 金属→绝缘体转变
- Mott (1940s 电子关联)
- Anderson (1970s localization via disorder)
- Slater (1951) antiferromagnetic AF order alone can open a gap regardless of the magnitude of the Coulomb interaction.
- Generally, a 3D conductor causes only a small fraction of changes in its electronic structure through the AF ordering 所以 Slater insulator 很少受到关注。

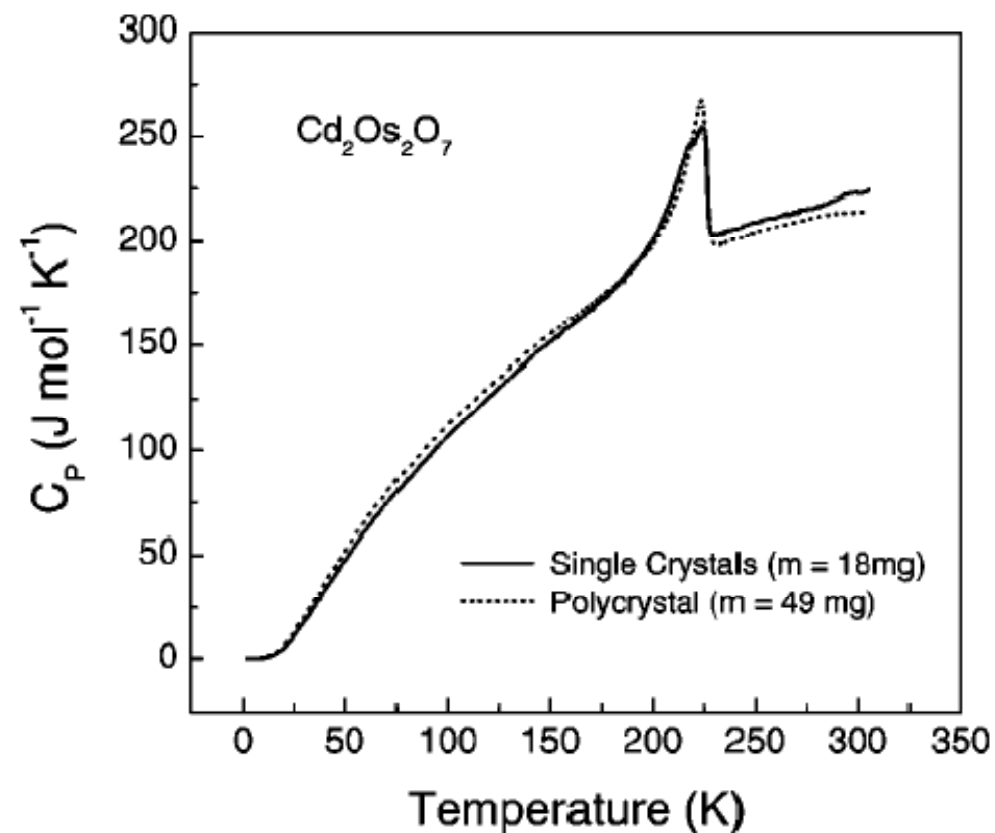
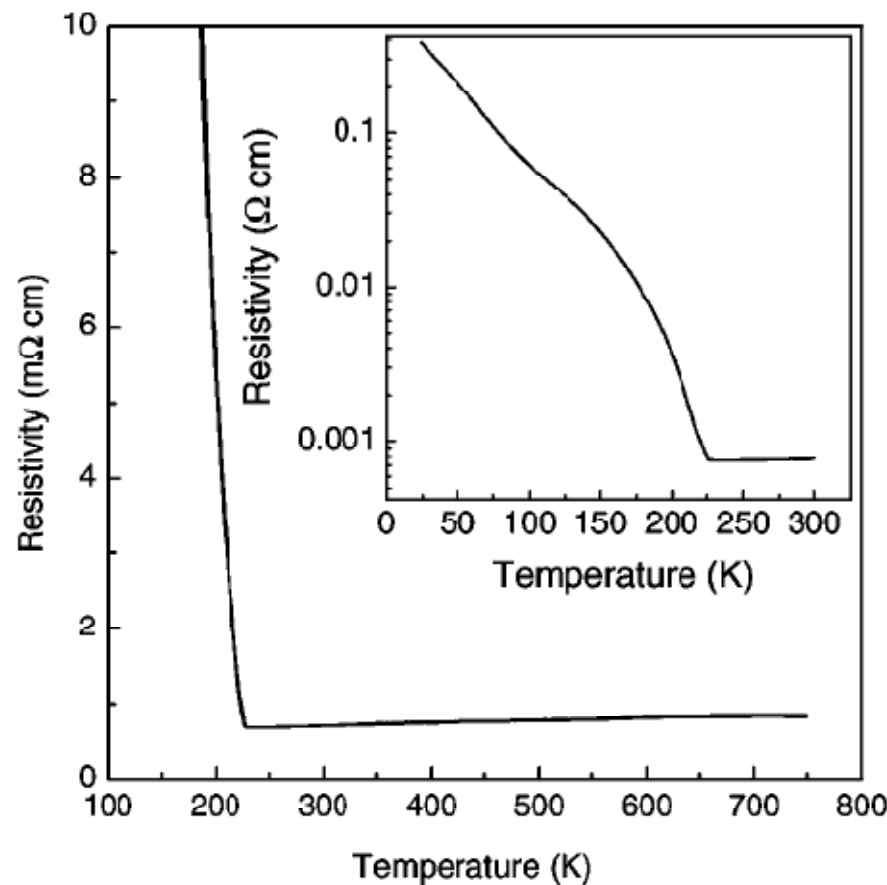
Slater Insulator $\text{Cd}_2\text{Os}_2\text{O}_7$

PHYSICAL REVIEW B, VOLUME 63, 195104

(2001)

Continuous metal-insulator transition in the pyrochlore $\text{Cd}_2\text{Os}_2\text{O}_7$

D. Mandrus,^{1,2,*} J. R. Thompson,^{2,1} R. Gaal,³ L. Forro,³ J. C. Bryan,⁴ B. C. Chakoumakos,¹ L. M. Woods,^{2,1} B. C. Sales,
R. S. Fishman,¹ and V. Keppens^{1,†}



All-in/all-out非共线磁结构

PRL 108, 247204 (2012)

PHYSICAL REVIEW LETTERS

week ending
15 JUNE 2012

Noncollinear Magnetism and Spin-Orbit Coupling in 5d Pyrochlore Oxide $\text{Cd}_2\text{Os}_2\text{O}_7$

We investigate the electronic and magnetic properties of the pyrochlore oxide $\text{Cd}_2\text{Os}_2\text{O}_7$ using the density-functional theory plus on-site repulsion (U) method, and depict the ground-state phase diagram with respect to U . We conclude that the all-in-all-out noncollinear magnetic order is stable in a wide range of U . We also show that the easy-axis anisotropy arising from the spin-orbit coupling plays a significant role in stabilizing the all-in-all-out magnetic order. A *pseudogap* was observed near the transition between

PRL 108, 247205 (2012)

PHYSICAL REVIEW LETTERS

week ending
15 JUNE 2012

Tetrahedral Magnetic Order and the Metal-Insulator Transition in the Pyrochlore Lattice of $\text{Cd}_2\text{Os}_2\text{O}_7$

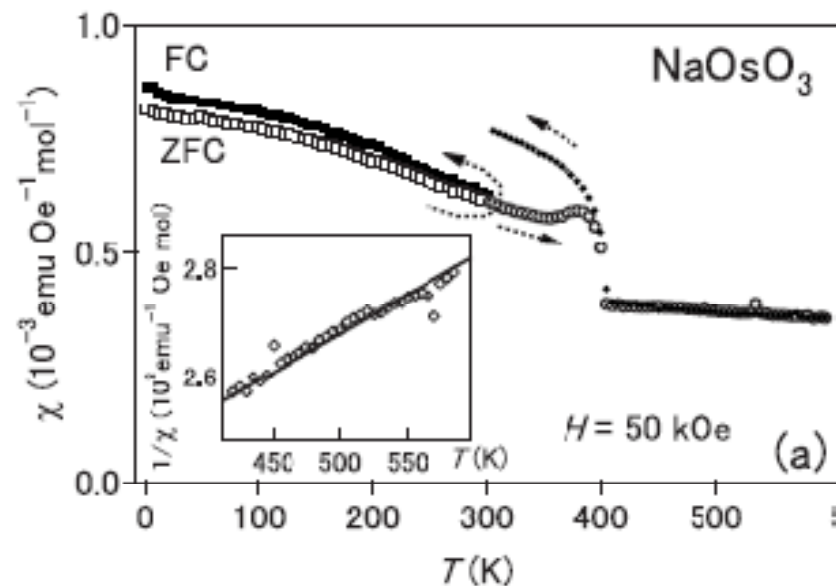
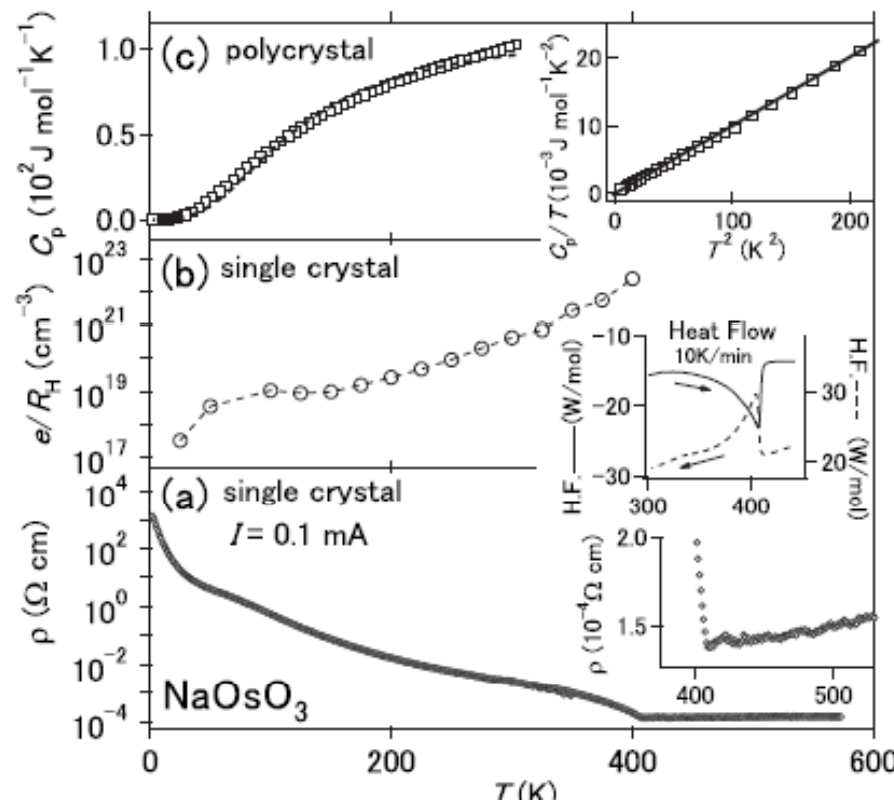
accompanied with any spatial symmetry breaking. We propose a noncollinear all-in-all-out spin arrangement on the tetrahedral network made of Os atoms. Based on this we suggest that the transition is not caused by the Slater mechanism as believed earlier but by an alternative mechanism related to the

NaOsO₃

PHYSICAL REVIEW B 80, 161104(R) (2009)

Continuous metal-insulator transition of the antiferromagnetic perovskite NaOsO₃

Y. G. Shi,^{1,2} Y. F. Guo,^{1,2} S. Yu,³ M. Arai,⁴ A. A. Belik,^{1,2} A. Sato,⁵ K. Yamaura,^{2,3,*} E. Takayama-Muromachi,^{1,2,3} H. F. Tian,⁶ H. X. Yang,⁶ J. Q. Li,⁶ T. Varga,⁷ J. F. Mitchell,⁷ and S. Okamoto⁸



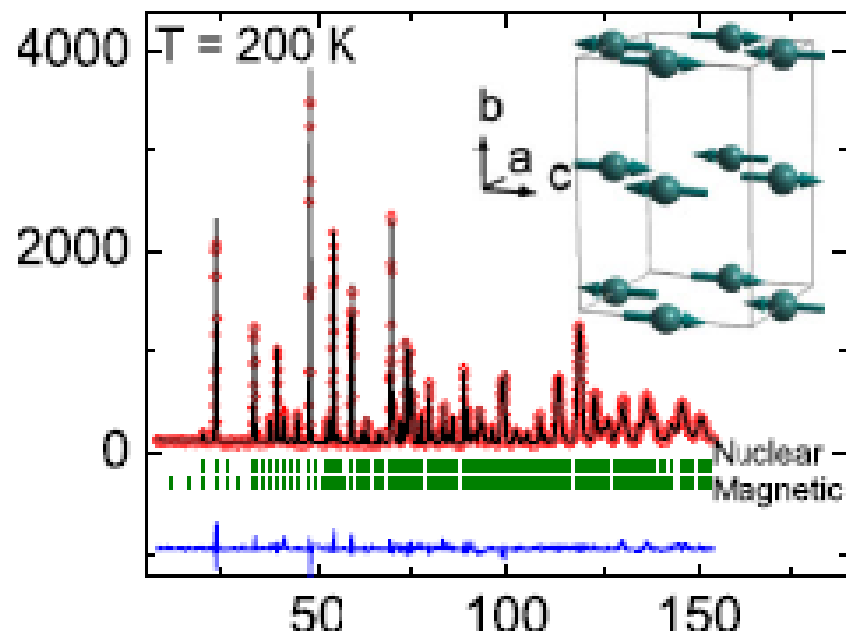
Electronic structure and magnetic properties of NaOsO₃

Yongping Du,¹ Xiangang Wan,^{1,2,*} Li Sheng,¹ Jinming Dong,¹ and Sergey Y. Savrasov²

- 1) Despite its big value the SOC has only weak effect on the band structure and magnetic moment.
- 2) The electronic correlations alone cannot open the band gap, and the low-temperature phase of NaOsO₃ is not a Mott-type insulator.
- 3) The magnetic configuration has an important effect on the conductivity, and the ground state is a **G-type AFM insulator**.
- 4) magnetic ordering → insulating behavior of NaOsO₃.
- 5) 磁化率曲线要小心

Magnetically Driven Metal-Insulator Transition in NaOsO_3

S. Calder,^{1,*} V. O. Garlea,¹ D. F. McMorrow,² M. D. Lumsden,¹ M. B. Stone,¹ J. C. Lang,³ J.-W. Kim,³ J. A. Schlueter,⁴ Y. G. Shi,^{5,6} K. Yamaura,⁶ Y. S. Sun,⁷ Y. Tsujimoto,⁷ and A. D. Christianson¹



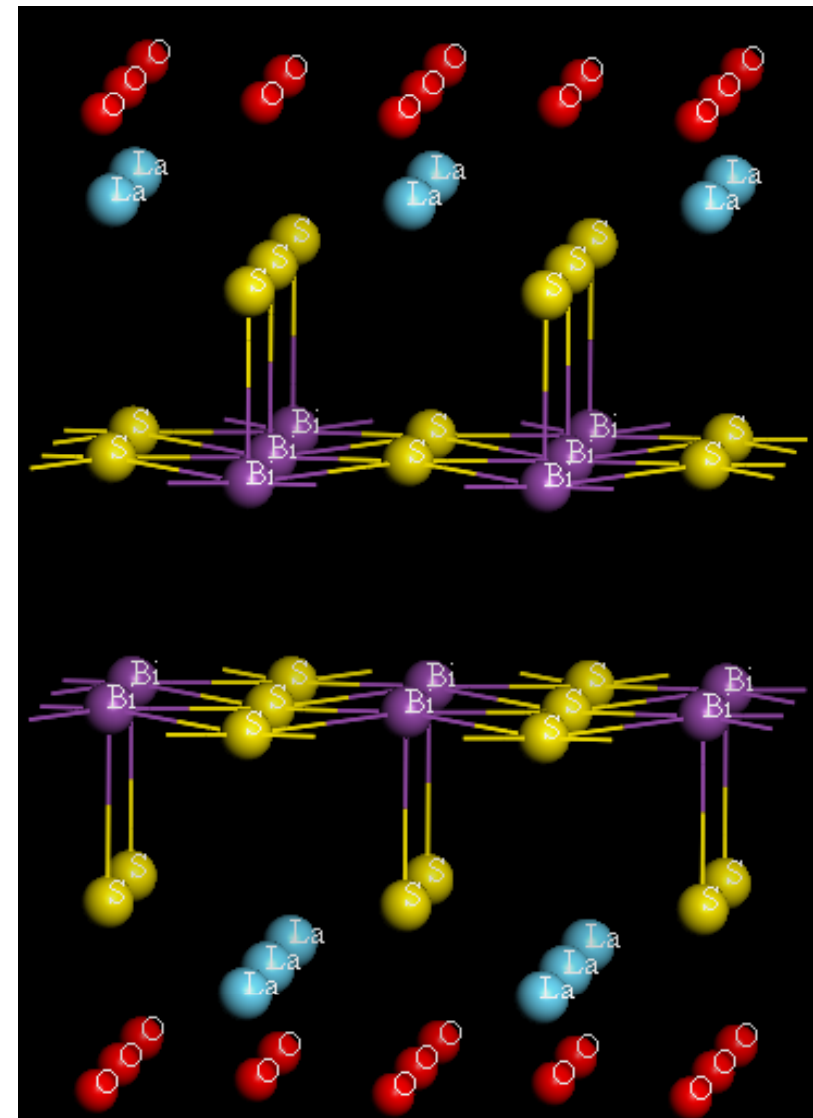
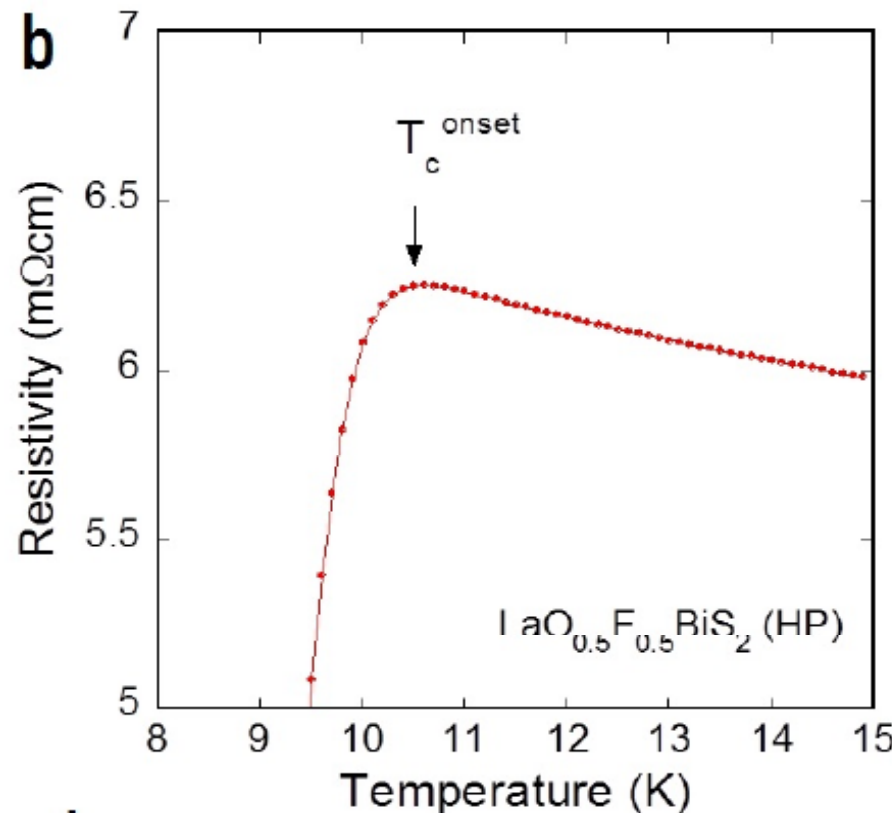
我们的理论结果被这篇实验很好的证实
磁矩大小，磁结构，SOC影响不大

主要的内容

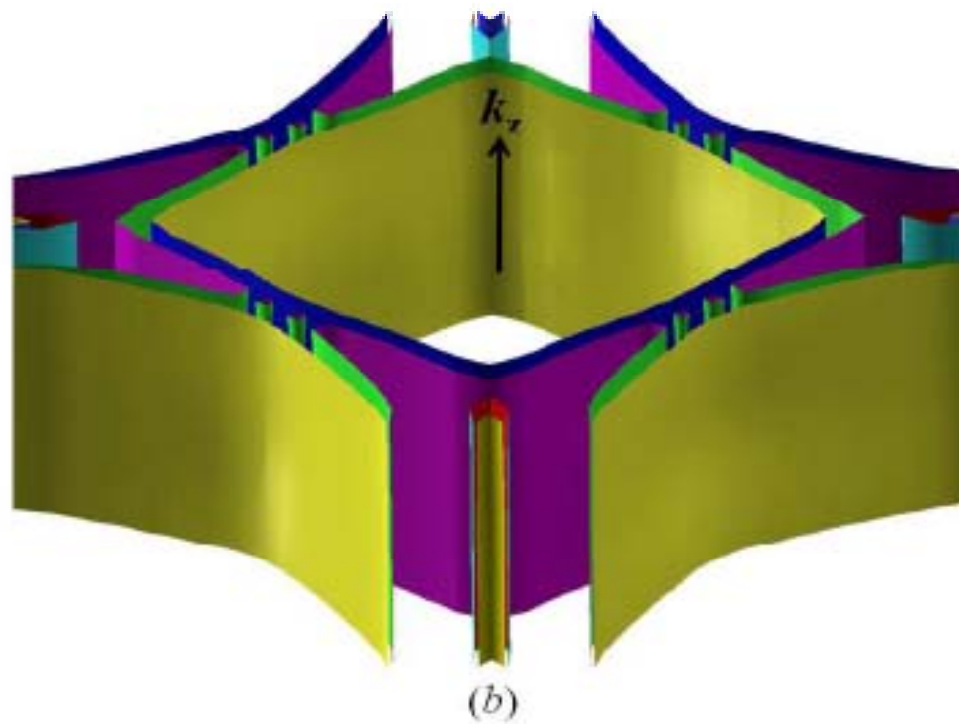
- 1) 烧绿石结构过渡金属Ir氧化物的磁结构
- 2) 对于金属也是可以对其拓扑分类的
- 3) Axion insulator
- 4) 确定了NaOsO₃是Slater insulator

BiS₂层状超导体 (2012-07)

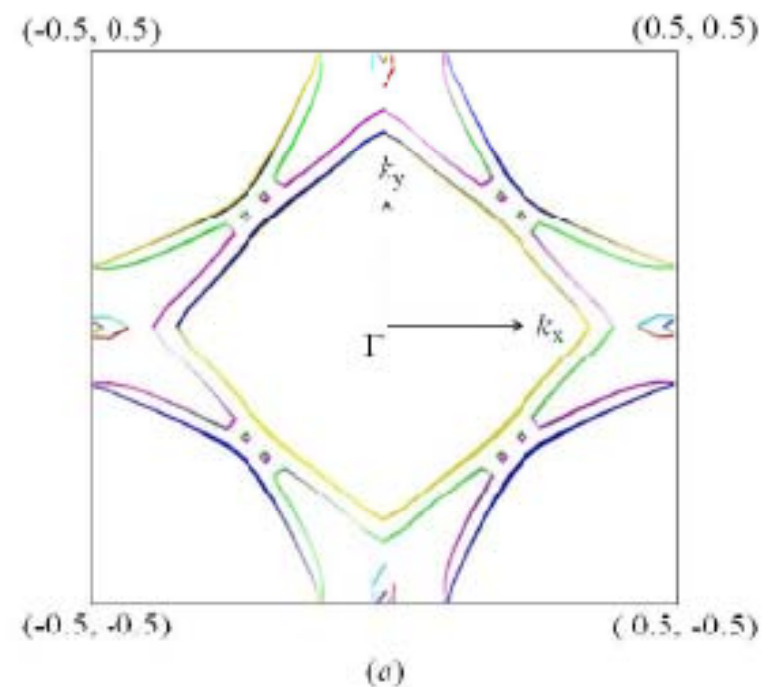
- Bi₄O₄S₃
- LaO_{1-x}F_xBiS₂
- NdOBiS₂



$\text{LaO}_{0.5}\text{F}_{0.5}\text{BiS}_2$ 的Fermi surface



(b)

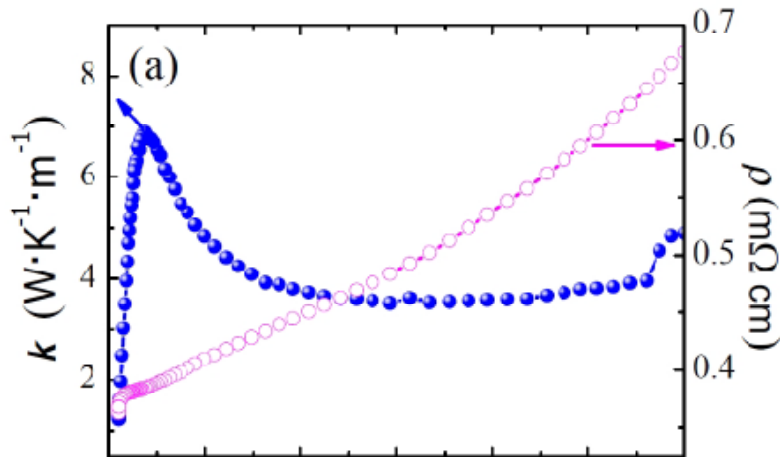


(a)

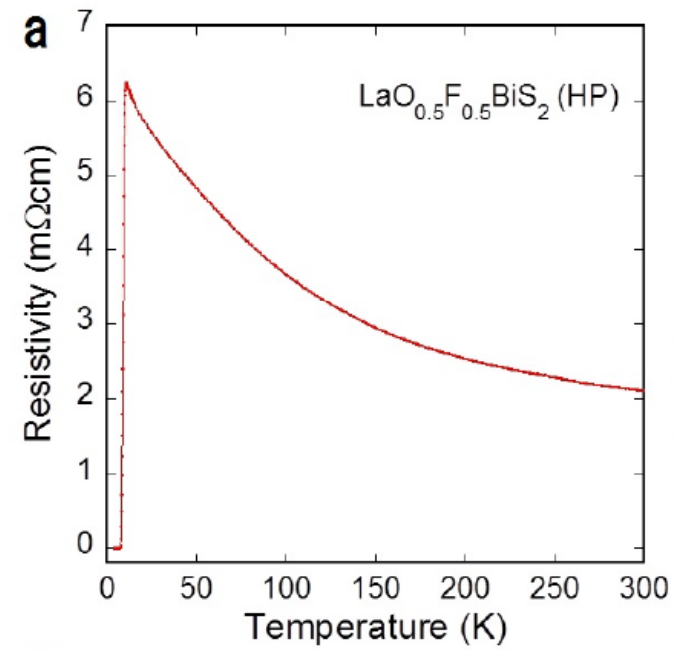
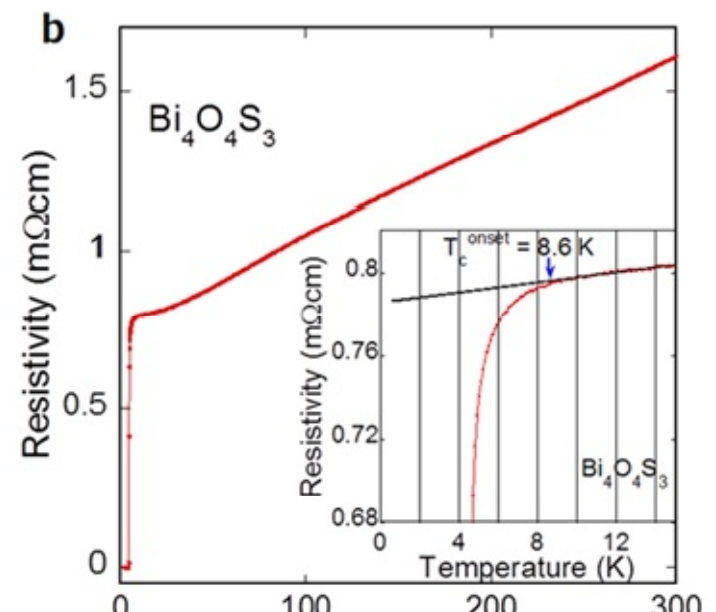
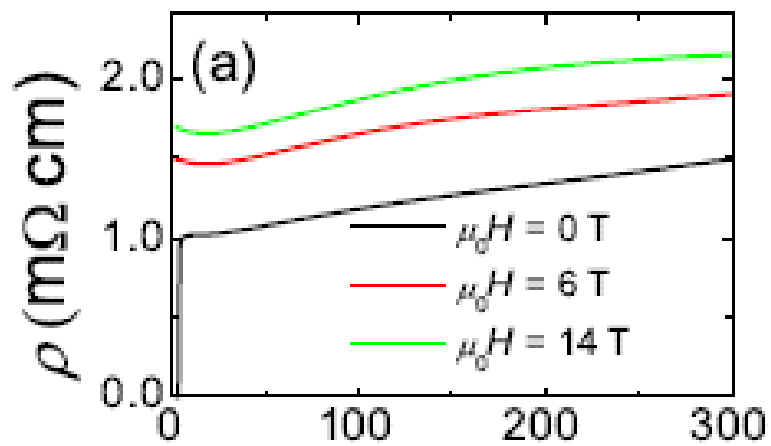
strong Fermi surface nesting at wavevectors
near $\mathbf{k} = (\pi, \pi, 0)$.

CDW?

Sun et al.,

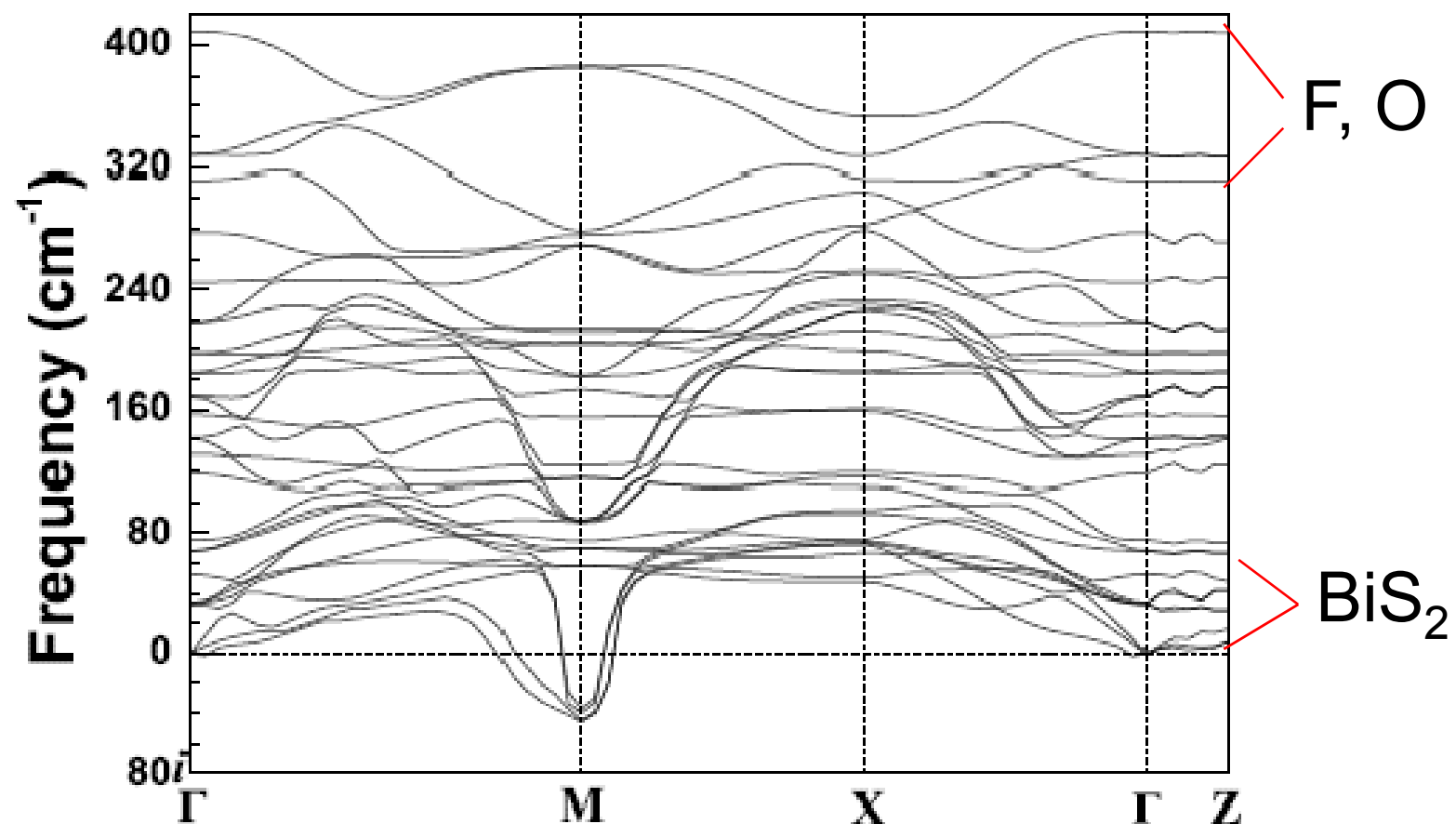


Wen et al.,

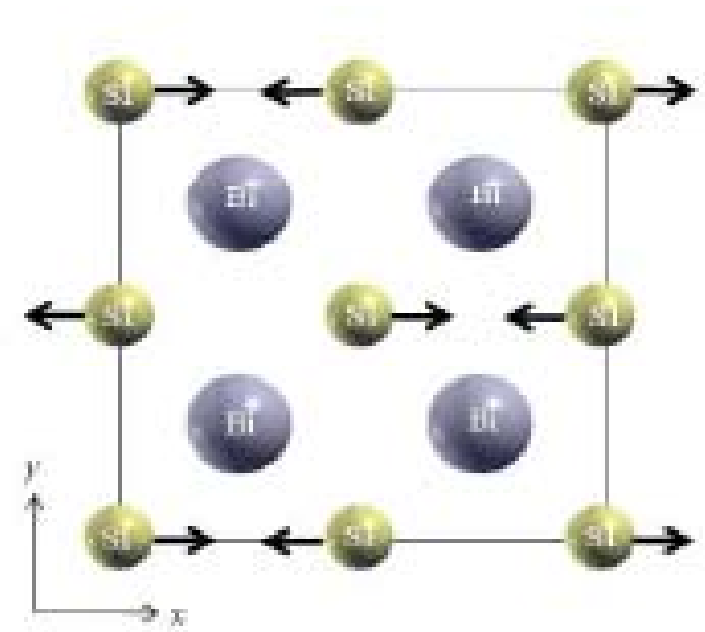
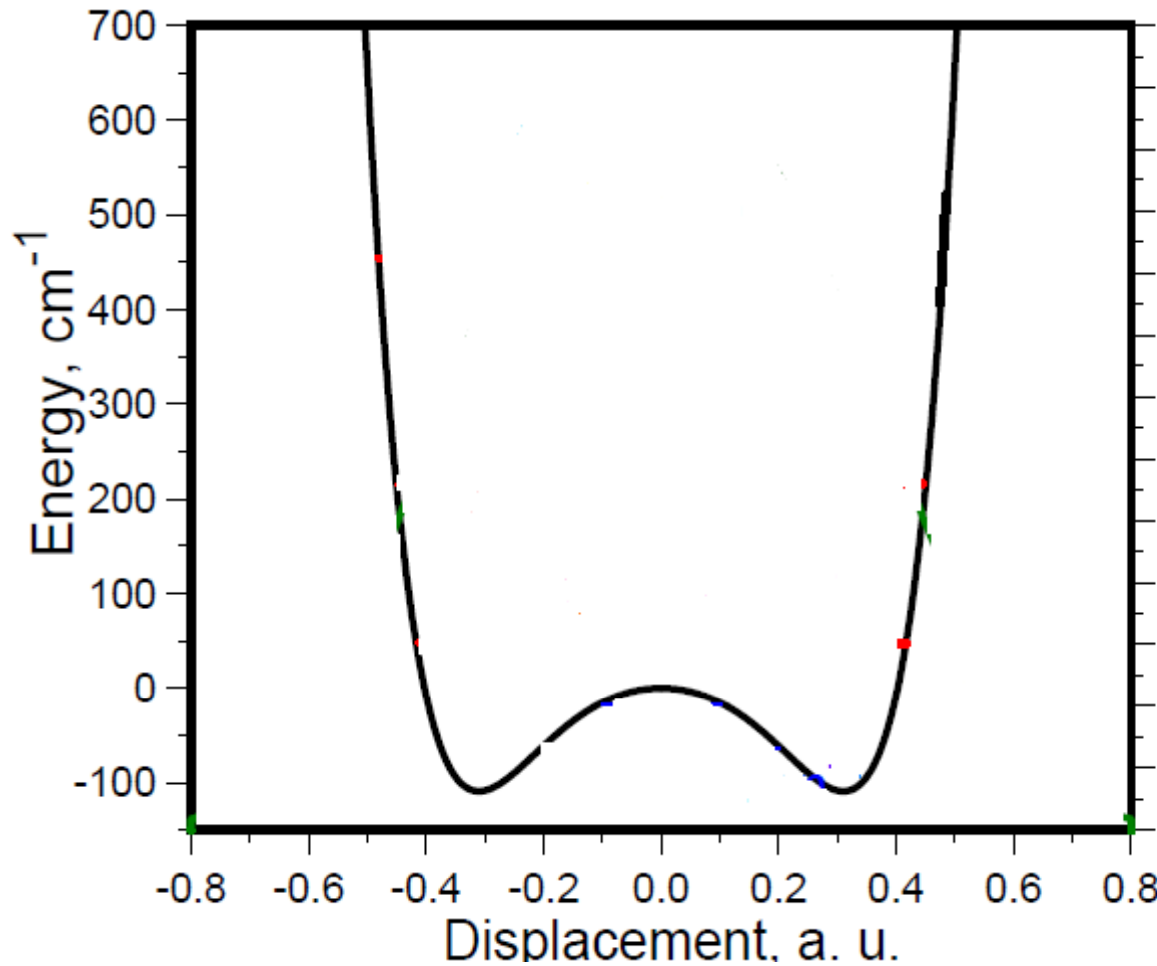


$\text{LaO}_{0.5}\text{F}_{0.5}\text{BiS}_2$ 的声子谱

linear response phonon calculation

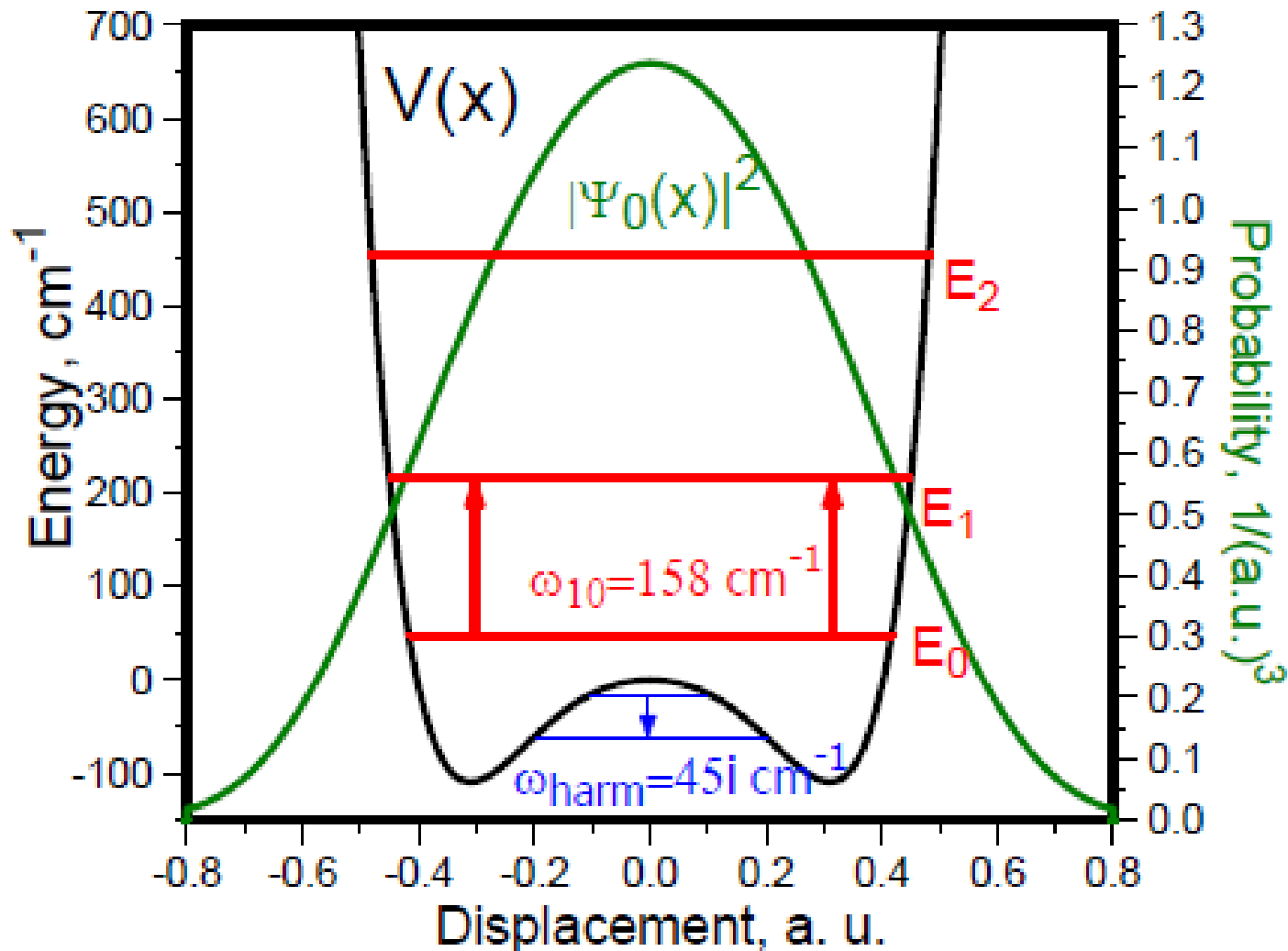


Frozen phonon calculation Nesting → CDW?



2套程序都得到了
double well

anharmonic problem



非谐的贡献

$$\frac{\Omega_n^2}{\Omega_0^2} \frac{M_{kk} |0\rangle^2}{E_n - E_0}$$

$\oplus \quad \square \quad N \otimes \cup \quad \begin{matrix} \Omega_n^2 \\ \odot \end{matrix} \quad \begin{matrix} \Omega_0^2 \\ \odot \end{matrix}$

$|0\rangle$ 是基态, $|n\rangle$ 是激发态

在谐波近视下 $E_n \approx E_0$ $n \odot \gamma_q$, γ_q 是声子能量

在非谐下 E_n 就不是 evenly spaced

Hui, Allen (1974)

electron-phonon interaction

- Four anharmonic modes

$$\tau_{total} \quad \blacksquare \quad 0.85$$

McMillan formula for T_c :

$$T_c = \frac{\Theta_D}{1.45} \exp \left[\frac{-1.04(1 + \lambda)}{\lambda(1 - 0.62\mu^*) - \mu^*} \right]$$

Coulomb parameter $\phi \quad \blacksquare \quad 0.1$

$$\gamma_D \quad \blacksquare \quad 260K$$

calculated $T_c \quad \blacksquare \quad 11.3K$

拓扑超导

Fu and Berg (PRL 2010)判据: **odd-parity pairing symmetry** and its Fermi surface encloses an odd number of time reversal invariant moments

已知的**拓扑+超导**的材料都是s/p电子体系

对于实际的材料体系 电声子耦合可能导致非常规超导吗?

BCS with General Pairing Symmetry

BCS gap equation

$$\Delta(\mathbf{k}) = - \sum_{\mathbf{k}'} W(\mathbf{kk}') \Delta(\mathbf{k}') \tanh\left(\frac{\epsilon_{\mathbf{k}'}}{2T_c}\right) / 2\epsilon_{\mathbf{k}'}$$

对于电声子耦合：

$$W(\mathbf{kj}\mathbf{k} + \mathbf{qj}') = |\langle \psi_{\mathbf{kj}} | \delta^{\mathbf{q}\nu} V_{eff} | \psi_{\mathbf{k+qj}'} \rangle|^2$$

线性响应密度泛函

$$V_{ext} \underset{R,t}{=} \frac{Ze^2}{|r - R - t_R|}$$

$$\nabla_{eff} \underset{\square}{=} \nabla_{ext} \underset{\square}{=} e^2 \underset{\times}{\square} \frac{\nabla}{|r - \square|} \underset{\square}{=} \frac{dV_{xc}}{d\nabla} \underset{\times}{\square}$$

$$\nabla^2 V_{eff} \underset{\square}{=} \nabla_{eff} \underset{\square}{\otimes} \nabla_{kj} \underset{\square}{\otimes} \nabla_{kj} \underset{\square}{=} \nabla_{eff} \nabla_{kj} \underset{\square}{=} 0$$

$$\nabla_{kj} \underset{\square}{\otimes} f_{kj} \nabla_{kj} \underset{\square}{\otimes} \nabla_{kj} \underset{\square}{=} h.c.$$

Orthonormalize polynomials at a given energy surface (such, e.g., as spherical harmonics in case of a sphere)

$$\frac{1}{N(\varepsilon)} \sum_{\mathbf{k}} \eta_a(\mathbf{k}) \eta_b(\mathbf{k}) \delta(\epsilon_{\mathbf{k}} - \varepsilon) = \delta_{ab}$$

Expanding superconducting energy gap and pairing interaction

$$\Delta(\mathbf{k}) = \sum_{\alpha} \Delta_a(\epsilon_{\mathbf{k}}) \eta_a(\mathbf{k}) \quad \Delta_a(\varepsilon) = \frac{1}{N(\varepsilon)} \sum_{\mathbf{k}} \delta(\epsilon_{\mathbf{k}} - \varepsilon) \Delta(\mathbf{k}) \eta_a^*(\mathbf{k})$$

$$W(\mathbf{kk}') = \sum_{\alpha\beta} W_{ab}(\epsilon_{\mathbf{k}} \epsilon_{\mathbf{k}'}) \eta_a(\mathbf{k}) \eta_b(\mathbf{k}')$$

$$W_{ab}(\varepsilon \varepsilon') = \frac{1}{N(\varepsilon) N(\varepsilon')} \sum_{\mathbf{kk}'} \delta(\epsilon_{\mathbf{k}} - \varepsilon) \eta_a^*(\mathbf{k}) W(\mathbf{kk}') \eta_b(\mathbf{k}') \delta(\epsilon_{\mathbf{k}'} - \varepsilon')$$

The gap equation becomes

$$\Delta_a(\varepsilon) = - \int d\varepsilon' \sum_b W_{ab}(\varepsilon \varepsilon') \Delta_b(\varepsilon') N(\varepsilon') \tanh\left(\frac{\varepsilon'}{2T_c}\right) / 2\varepsilon'$$

pairing occurs for the electrons within a thin layer near E_f

$$\Delta_a(\varepsilon) = \begin{cases} \Delta_a & \text{for } -\omega_D < \varepsilon < +\omega_D \\ 0 & \text{otherwise} \end{cases}$$

$$W_a(\varepsilon\varepsilon') = \begin{cases} W_a & \text{for } -\omega_D < \varepsilon < +\omega_D \\ 0 & \text{otherwise} \end{cases}$$

This reduces the gap equation to (integral is extended over Debye frequency range)

$$\Delta_a = -N(0) \sum_b W_{ab} \Delta_b \int_{-\omega_D}^{+\omega_D} d\varepsilon' \frac{1}{2\varepsilon'} \tanh\left(\frac{\varepsilon'}{2T_c}\right)$$

Assuming crystal symmetry makes $W_{ab} = W_a \delta_{ab}$ and evaluating the integral gives

$$T_c = 1.134 \omega_D e^{-1/\lambda_a} \quad \lambda_a = -N(0)W_a$$

where the average electron-phonon coupling in a given a channel is given by the Fermi surface average of the electron-phonon coupling

$$W_a = \frac{1}{N(0)N(0)} \sum_{\mathbf{k}\mathbf{k}'} \delta(\epsilon_{\mathbf{k}}) \eta_a(\mathbf{k}) W(\mathbf{k}\mathbf{k}') \eta_a(\mathbf{k}') \delta(\epsilon_{\mathbf{k}'})$$

Finally, the superconducting state with largest λ_a will be realized.

为何实际材料电声子耦合总是s-wave like?

电声子耦合往往是实空间局域的 $W(\mathbf{k}, \mathbf{k}')$ 基本与 \mathbf{k} 无关

$$\lambda_a = -\frac{1}{N(0)} \sum_{\mathbf{k}\mathbf{k}'} \delta(\epsilon_{\mathbf{k}}) \eta_a(\mathbf{k}) W(\mathbf{k}\mathbf{k}') \eta_a(\mathbf{k}') \delta(\epsilon_{\mathbf{k}'})$$

In the extreme case $W(\mathbf{k}, \mathbf{k}') = W_0$ we obtain:

$$\lambda_a = -W_0 N(0) \delta_{a=s-wave}$$

所以只有s-wave!

另外一个极限：电声子耦合在k空间局域

$$W(\mathbf{k}, \mathbf{k}') = W_1 \delta(\mathbf{k} - \mathbf{k}' - \mathbf{q}_0) = W_1 \sum_a \eta_a(\mathbf{k}) \eta_a(\mathbf{k}' + \mathbf{q}_0)$$

$$\lambda_a = -W_1 \sum_{\mathbf{k}} \delta(\epsilon_{\mathbf{k}}) \eta_a(\mathbf{k}) \eta_a(\mathbf{k} + \mathbf{q}_0) = -W_1 N(0) O_a(\mathbf{q}_0)$$

where the overlap matrix between two polynomials shows up

$$O_a(\mathbf{q}_0) = \frac{1}{N(0)} \sum_{\mathbf{k}} \delta(\epsilon_{\mathbf{k}}) \eta_a(\mathbf{k}) \eta_a(\mathbf{k} + \mathbf{q}_0)$$

It would be less than unity for non-zero angular momentum index a unless $\mathbf{q}_0 \Rightarrow 0$

$$\lim_{q_0 \rightarrow 0} O_a(\mathbf{q}_0) = 1$$

实际材料电声子耦合只能s-wave吗？

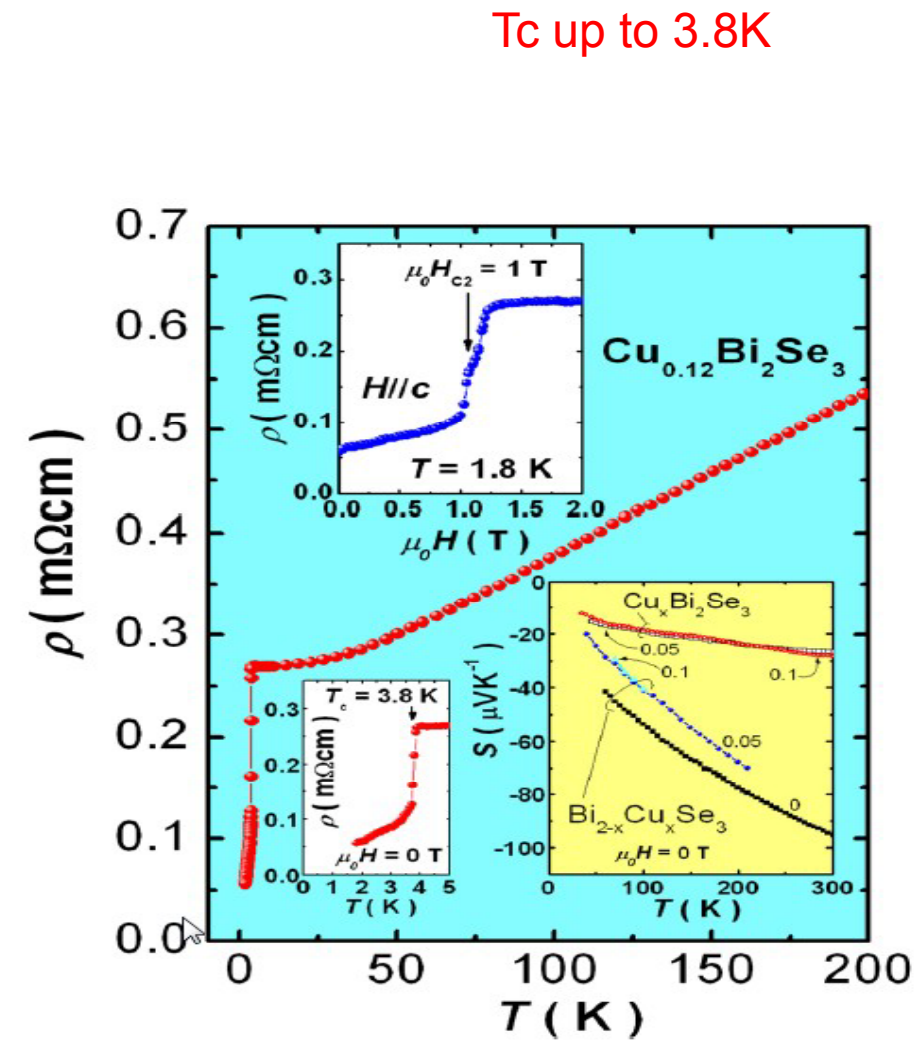
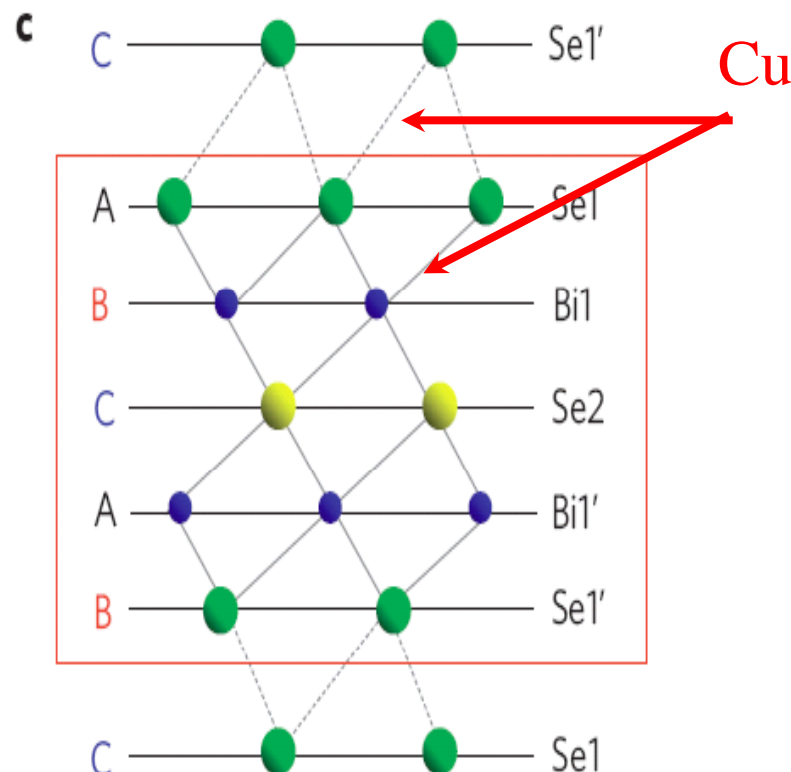
要找电声子耦合在倒空间局域

需要 

LDA+SO → Bi_2Se_3 !

Superconductivity in $\text{Cu}_x\text{Bi}_2\text{Se}_3$

Hor et al, PRL 104, 057001 (2010)



Symmetry of Pairing State

- Point-contact spectroscopy: odd-parity pairing in $\text{Cu}_x\text{Bi}_2\text{Se}_3$ (Sasaki et.al, PRL 2011) via observed zero-bias conductance

PRL 107, 217001 (2011)

PHYSICAL REVIEW LETTERS

week ending
18 NOVEMBER 2011

Topological Superconductivity in $\text{Cu}_x\text{Bi}_2\text{Se}_3$

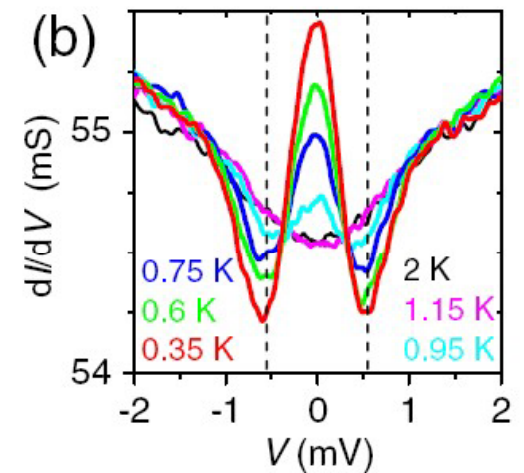
Satoshi Sasaki,¹ M. Kriener,¹ Kouji Segawa,¹ Keiji Yada,² Yukio Tanaka,² Masatoshi Sato,³ and Yoichi Ando^{1,*}

¹Institute of Scientific and Industrial Research, Osaka University, Ibaraki, Osaka 567-0047, Japan

²Department of Applied Physics, Nagoya University, Nagoya 464-8603, Japan

³Institute for Solid State Physics, University of Tokyo, Chiba 277-8581, Japan

(Received 2 August 2011; published 14 November 2011)



- Scanning-tunneling spectroscopy: fully gapped state in $\text{Cu}_x\text{Bi}_2\text{Se}_3$

PRL 110, 117001 (2013)

PHYSICAL REVIEW LETTERS

week ending
15 MARCH 2013



Experimental Evidence for *s*-Wave Pairing Symmetry in Superconducting $\text{Cu}_x\text{Bi}_2\text{Se}_3$ Single Crystals Using a Scanning Tunneling Microscope

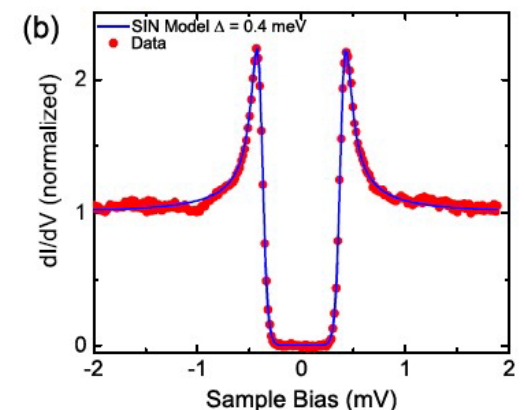
Niv Levy,^{1,2} Tong Zhang,^{1,2} Jeonghoon Ha,^{1,2,3} Fred Sharifi,¹ A. Alec Talin,¹ Young Kuk,³ and Joseph A. Stroscio^{1,*}

¹Center for Nanoscale Science and Technology, NIST, Gaithersburg, Maryland 20899, USA

²Maryland NanoCenter, University of Maryland, College Park, Maryland 20742, USA

³Department of Physics and Astronomy, Seoul National University, Seoul 151-747, Korea

(Received 1 November 2012; published 12 March 2013)



Pressure-Induced Unconventional Superconducting Phase in the Topological Insulator Bi_2Se_3

Kevin Kirshenbaum,¹ P. S. Syers,¹ A. P. Hope,¹ N. P. Butch,² J. R. Jeffries,² S. T. Weir,² J. J. Hamlin,³ M. B. Maple,³ Y. K. Vohra,⁴ and J. Paglione^{1,*}

¹*Department of Physics, Center for Nanophysics and Advanced Materials, University of Maryland,
College Park, Maryland 20742, USA*

²*Condensed Matter and Materials Division, Lawrence Livermore National Laboratory, Livermore, California 94550, USA*

³*Department of Physics, University of California, San Diego, La Jolla, California 92093, USA*

⁴*Department of Physics, University of Alabama at Birmingham, Birmingham, Alabama 35294, USA*

(Received 26 February 2013; published 20 August 2013)

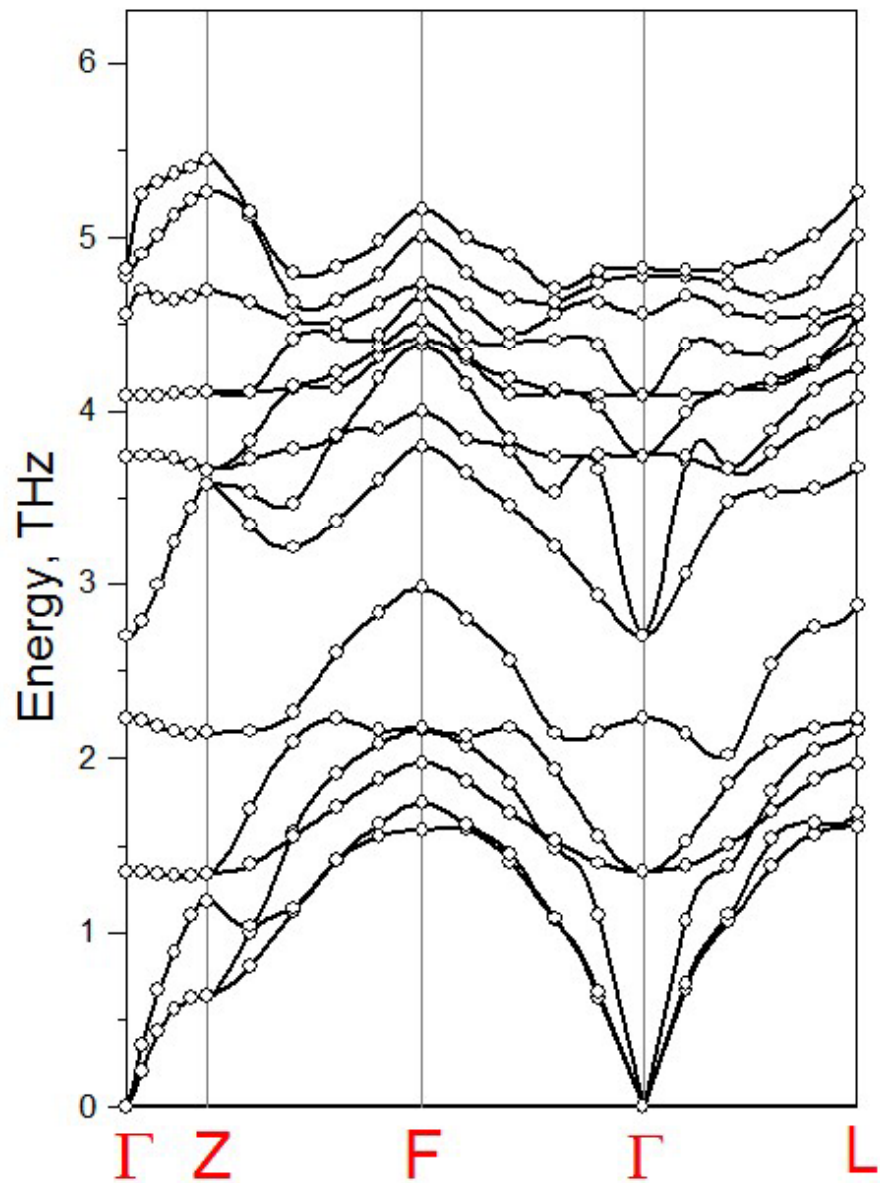
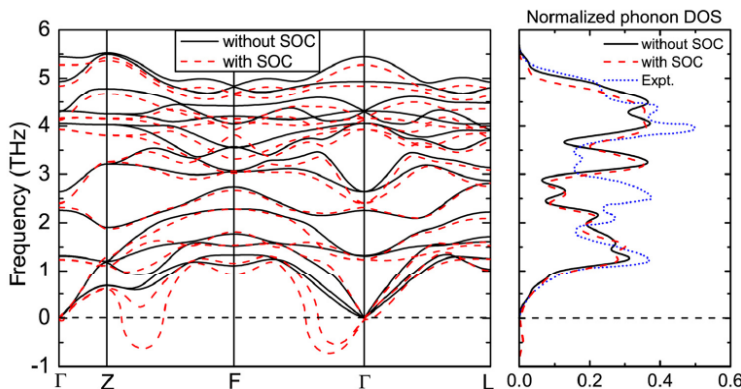
Simultaneous low-temperature electrical resistivity and Hall effect measurements were performed on single-crystalline Bi_2Se_3 under applied pressures up to 50 GPa. As a function of pressure, superconductivity is observed to onset above 11 GPa with a transition temperature T_c and upper critical field H_{c2} that both increase with pressure up to 30 GPa, where they reach maximum values of 7 K and 4 T, respectively. Upon further pressure increase, T_c remains anomalously constant up to the highest achieved pressure. Conversely, the carrier concentration increases continuously with pressure, including a tenfold increase over the pressure range where T_c remains constant. Together with a quasilinear temperature dependence of H_{c2} that exceeds the orbital and Pauli limits, the anomalously stagnant pressure dependence of T_c points to an unconventional pressure-induced pairing state in Bi_2Se_3 that is unique among the superconducting topological insulators.

Phonon Spectrum for Bi_2Se_3

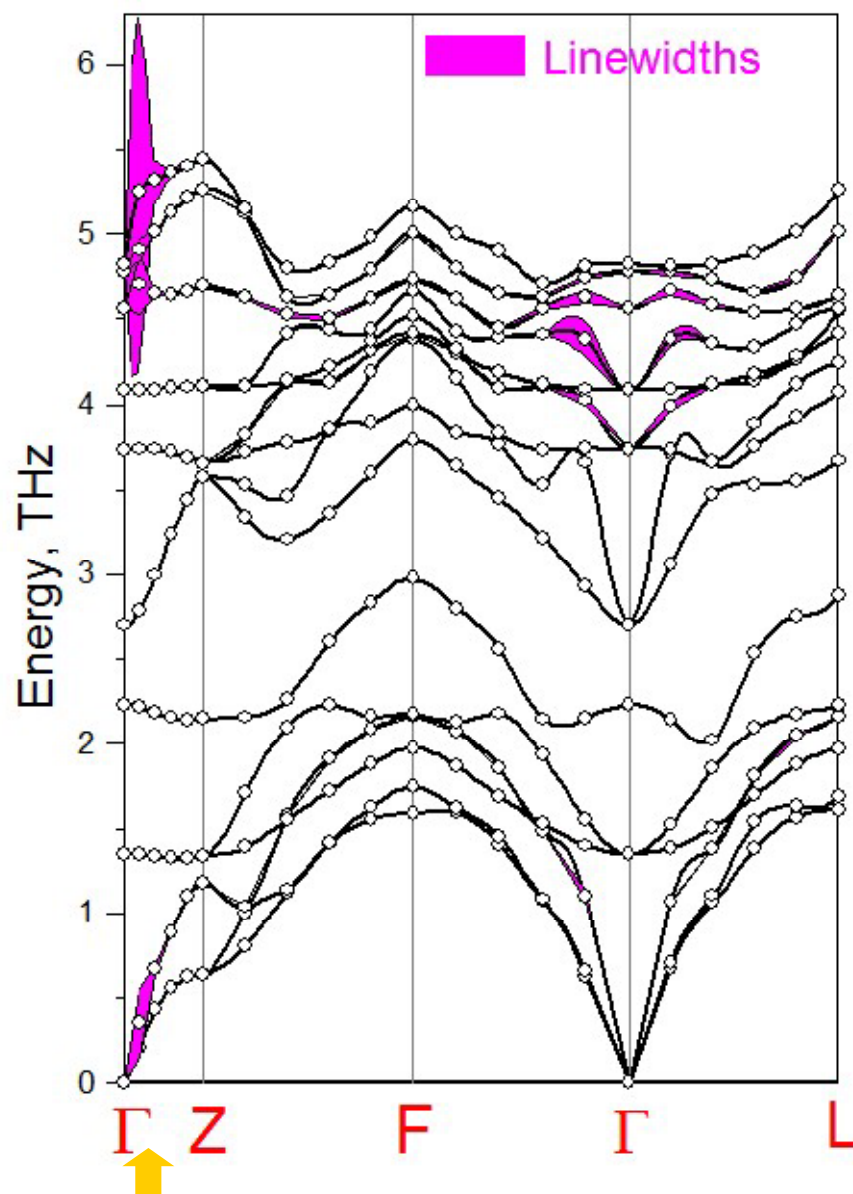
Density functional linear response approach

LDA+SO

Prior VASP calculations in
Appl. Phys. Lett. **100**, 082109 (2012)
reported some instabilities which
we did not confirm



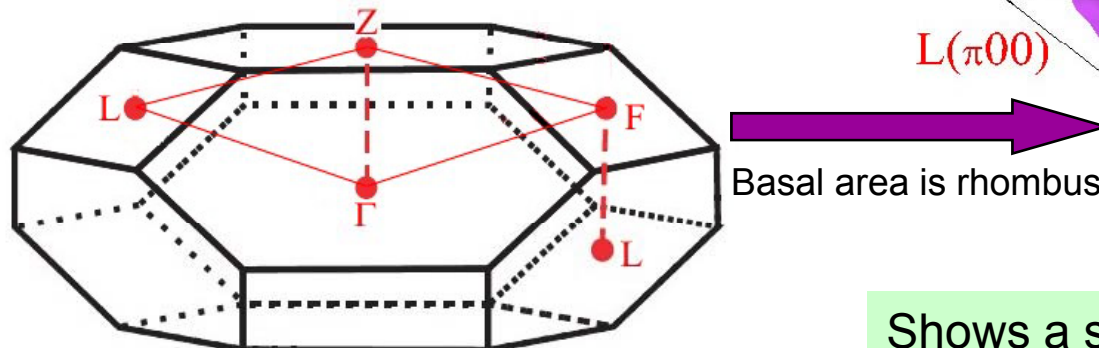
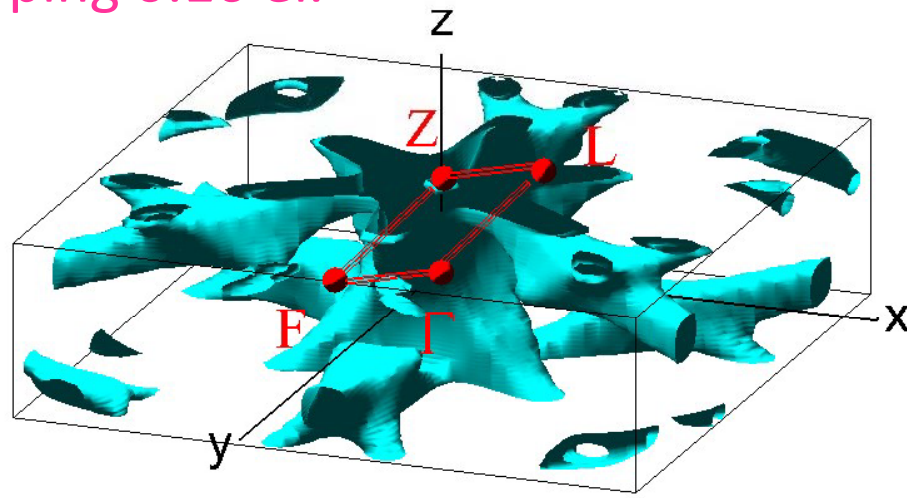
Calculated phonon linewidths in doped Bi₂Se₃



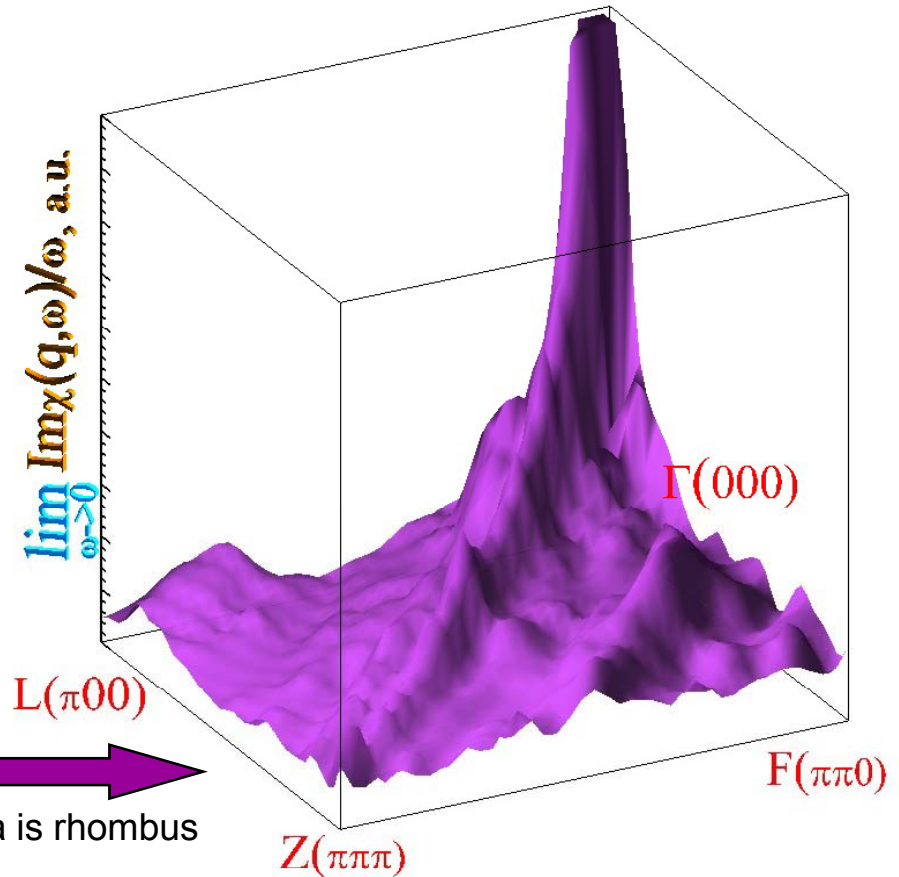
Electron-phonon coupling is enormous at $\mathbf{q}_0 \sim (0,0,0.04)2\pi/c$

Nesting Function

Doping 0.16 el.



$$\chi(\mathbf{q}) = \sum_{\mathbf{k}} \delta(\epsilon_{\mathbf{k}}) \delta(\epsilon_{\mathbf{k}+\mathbf{q}})$$

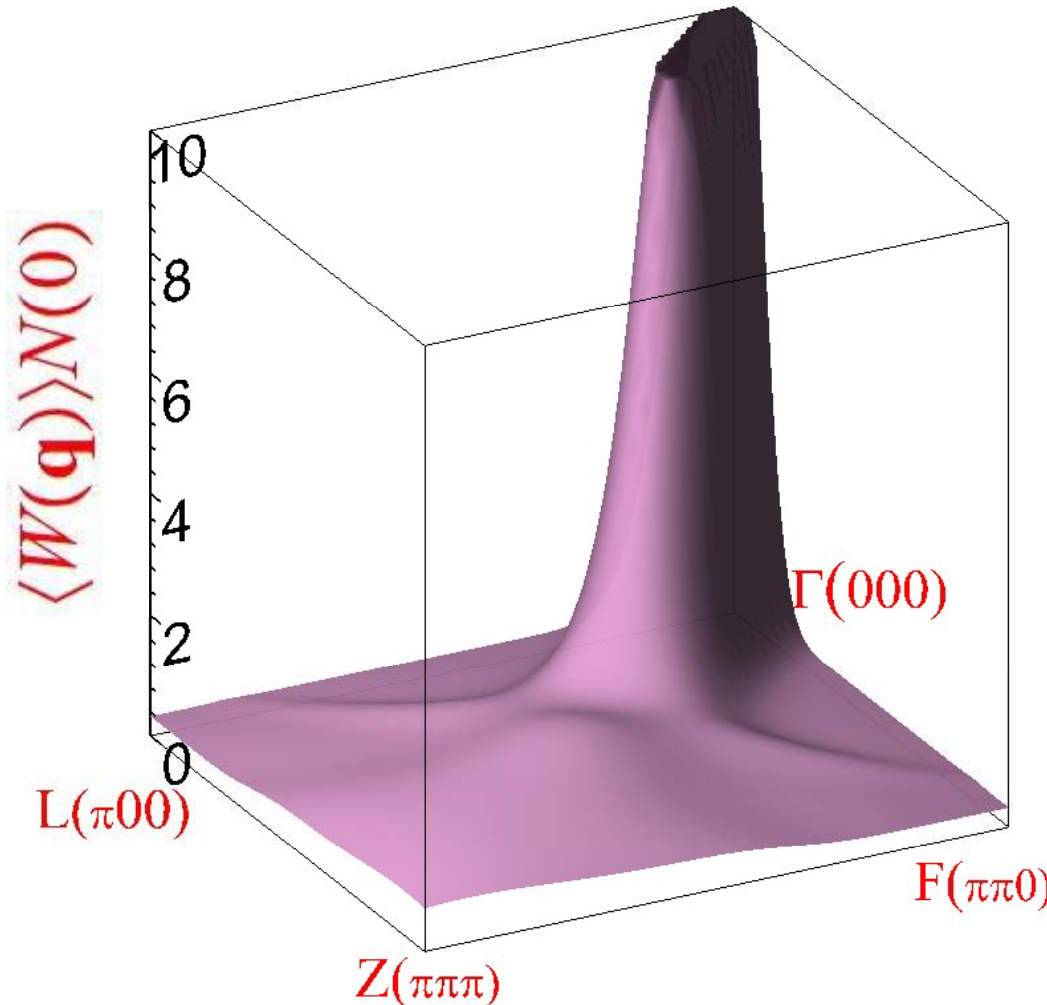


Shows a strong ridge-like structure along ΓZ line at small \mathbf{q} 's due to quasi 2D features of the Fermi surface.

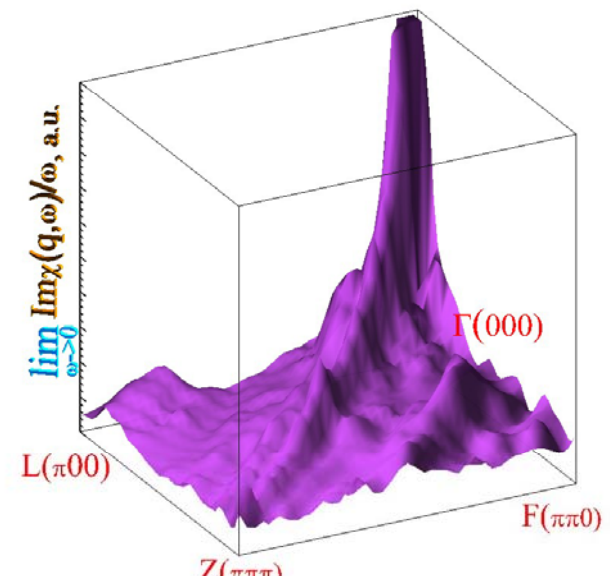
Calculated electron-phonon matrix elements

Define average electron-phonon matrix element (squared) as follows

$$\langle W(\mathbf{q}) \rangle = \frac{\sum_{\mathbf{k}} W(\mathbf{k}, \mathbf{k} + \mathbf{q}) \delta(\epsilon_{\mathbf{k}}) \delta(\epsilon_{\mathbf{k}+\mathbf{q}})}{\sum_{\mathbf{k}} \delta(\epsilon_{\mathbf{k}}) \delta(\epsilon_{\mathbf{k}+\mathbf{q}})}$$

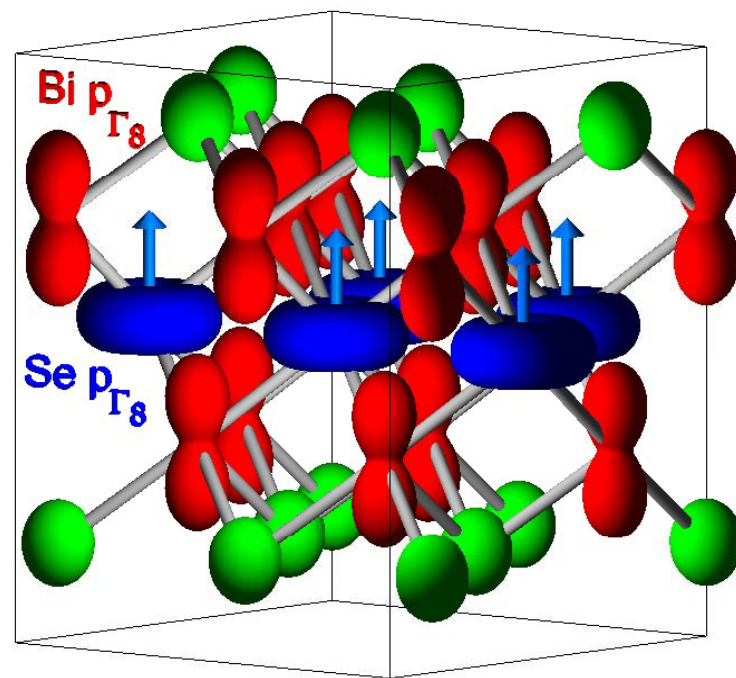
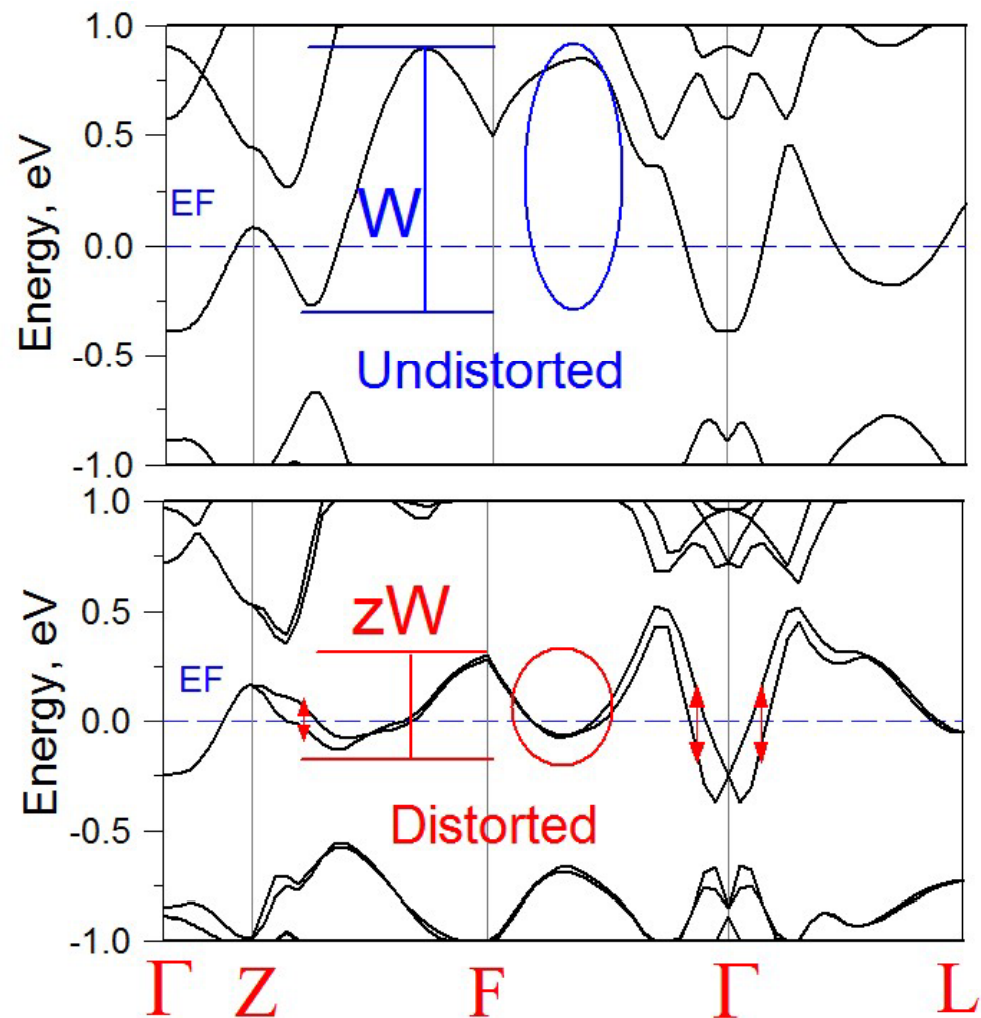


This eliminates all nesting-like features of $\chi(\mathbf{q}) = \sum_{\mathbf{k}} \delta(\epsilon_{\mathbf{k}}) \delta(\epsilon_{\mathbf{k}+\mathbf{q}})$



Still $\langle W(\mathbf{q}) \rangle$ shows almost singular behavior for $\mathbf{q}_0 \sim (0, 0, 0.04) 2\pi/c$

Calculated deformation potentials at long wavelengths



自旋轨道耦合

中心反演对称

强的自旋轨道耦合在此很重要

打破中心反演对称

Basis function for hexagonal lattices

PHYSICAL REVIEW B

VOLUME 37, NUMBER 4

1 FEBRUARY 1988

Stability of anisotropic superconducting phases in UPt₃

W. Putikka and Robert Joynt

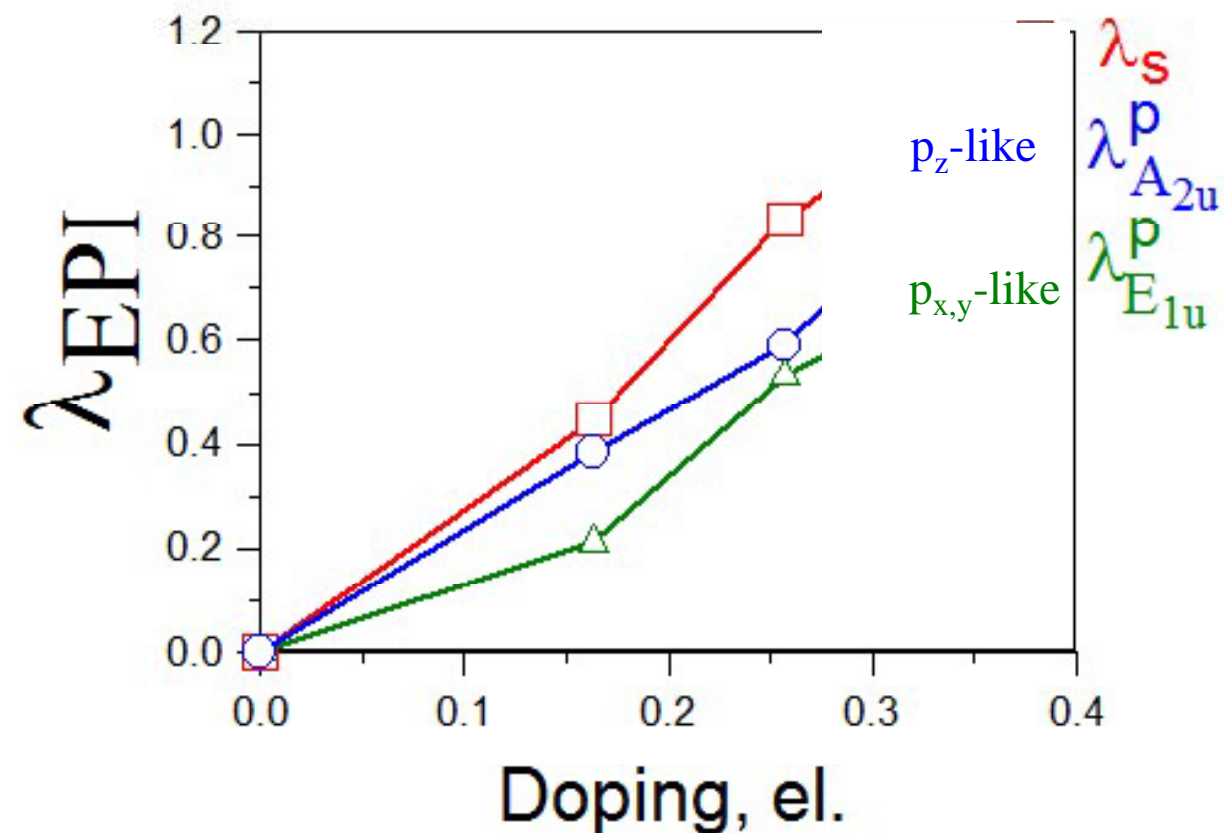
Physics Department, 1150 University Avenue, University of Wisconsin-Madison, Madison, Wisconsin 53706

(Received 26 October 1987)

TABLE I. Basis functions for the various representations of D_6 . The interaction can be decomposed into sums of products of these functions.

Representation	Function
A_{1g}	$\phi_k = \frac{1}{\sqrt{3}} \cos\left(\frac{ck_z}{2}\right) \left[\cos\left(\frac{\sqrt{3}ak_y}{3}\right) + \cos\left(\frac{ak_x}{2} + \frac{\sqrt{3}ak_y}{6}\right) + \cos\left(\frac{ak_x}{2} - \frac{\sqrt{3}ak_y}{6}\right) \right]$
B_{1g}	$\psi_k = \frac{1}{\sqrt{3}} \sin\left(\frac{ck_z}{2}\right) \left[\sin\left(\frac{\sqrt{3}ak_y}{3}\right) + \sin\left(\frac{ak_x}{2} - \frac{\sqrt{3}ak_y}{6}\right) - \sin\left(\frac{ak_x}{2} + \frac{\sqrt{3}ak_y}{6}\right) \right]$
E_{1g}	$\theta_k = \frac{1}{\sqrt{2}} \sin\left(\frac{ck_z}{2}\right) \left[\sin\left(\frac{ak_x}{2} + \frac{\sqrt{3}ak_y}{6}\right) + \sin\left(\frac{ak_x}{2} - \frac{\sqrt{3}ak_y}{6}\right) \right]$
	$\xi_k = \frac{1}{\sqrt{6}} \sin\left(\frac{ck_z}{2}\right) \left[2 \sin\left(\frac{\sqrt{3}ak_y}{3}\right) + \sin\left(\frac{ak_x}{2} + \frac{\sqrt{3}ak_y}{6}\right) - \sin\left(\frac{ak_x}{2} - \frac{\sqrt{3}ak_y}{6}\right) \right]$

Large Electron-Phonon Interaction in $\text{Cu}_x\text{Bi}_2\text{Se}_3$



S-wave shows largest coupling. P-wave is also very large!

Coulomb pseudopotential μ^* 压制 s-wave

$$T_c^{(l)} = 1.14\omega_D \exp\left(-\frac{1}{\lambda_l^{eff}}\right)$$

$$\lambda_l^{eff} = \frac{\lambda_l - \mu_l^*}{1 + \lambda_{s-h}} \quad \mu_l^* = \frac{\mu_l}{1 + \mu_l \ln \epsilon_F / \omega_D}$$

where μ_l is the Fermi surface average of the screened Coulomb interaction

$$\mu_l = \frac{1}{N(0)} \sum_{\mathbf{k}\mathbf{k}'} \langle \mathbf{k} - \mathbf{k} | U | \mathbf{k}' - \mathbf{k}' \rangle \delta(\epsilon_{\mathbf{k}}) \delta(\epsilon_{\mathbf{k}'}) \eta_l(\mathbf{k}) \eta_l(\mathbf{k}')$$

Assuming Hubbard like on-site Coulomb repulsion

$$\langle \mathbf{k} - \mathbf{k} | U | \mathbf{k}' - \mathbf{k}' \rangle = U$$

μ^* will affect s-wave pairing only

$$\mu_{l=s} = UN(0) \quad \mu_{l>s} = 0$$

Estimates with μ^*

For doped Bi_2Se_3 we obtain the estimate

$$\omega_D \sim 100K$$

$$\varepsilon_F \sim 2000 - 5000K$$

and

$$\mu_s^* = 0.1$$

For doping by 0.16 electrons we get the estimates

S-wave

$$\lambda_s^{EPI} = 0.45$$

$$\mu_s^* = 0.1$$

P-wave

$$\lambda_{A_{2u}}^{EPI} = 0.39$$

$$\mu_{l>s}^* \sim 0$$

Effective coupling $\lambda - \mu^*$ for p-wave pairing channel wins!

Other Compounds

Bi_2Te_3

TlBiTe_2

Doped-SnTe

Conclusion

- Large electron-phonon coupling is found for $\text{Cu}_x\text{Bi}_2\text{Se}_3$
- Not only s-wave but also p-wave pairing is found to be large due to strong anisotropy and quasi-2D Fermi surfaces. $\lambda_s \sim \lambda_p$
- Coulomb interaction and spin fluctuations will reduce λ_s and make $\lambda_p > \lambda_s$ therefore unconventional superconductivity may indeed be realized here.
- Discussed effects have nothing to do with topological aspect of the problem, may be found in other doped band insulators.

谢 谢